[American Journal of Science, Vol. 306, December, 2006, P. 846–873, DOI 10.2475/10.2006.03]

THERMOCHRONOLOGY OF THE WEST SUDETES (BOHEMIAN MASSIF): RAPID AND REPEATED EDUCTION IN THE EASTERN VARISCIDES, POLAND AND CZECH REPUBLIC

D. A. SCHNEIDER*, S. J. ZAHNISER*, J. M. GLASCOCK*, S. M. GORDON**, and M. MANECKI***

ABSTRACT. The Sudete Mountains of northeastern Bohemian Massif were amalgamated during the closure of the Rheic ocean, culminating with Variscan orogenesis, and contain occurrences of high-pressure granulite and small relict ultrahigh-pressure eclogite formed during subduction. We performed $^{40}Ar/^{39}Ar$ thermochronometry on primarily amphibolite-facies gneisses and schists from two crustal blocks within the Sudetes: Góry Sowie and Orlica-Snieznik massifs. Hornblende and mica plateau ages from the mountainous portion of the Góry Sowie reflect relatively rapid cooling between 382 ± 1 Ma and 373 ± 0.5 Ma, following peak conditions at ca. 400 Ma. Kyanite-sillimanite and cordierite-garnet mineral growth textures denote near isothermal decompression during eduction. Concordant hornblende and biotite cooling ages obtained from the eastern, topographically flat region adjacent to the Niemcza shear zone indicate markedly younger cooling at 337 ± 0.8 Ma. $^{40}Ar/^{39}Ar$ results from the Snieznik Mountains, 50 km to the south, yield plateau cooling ages for white mica and biotite between 341 ± 1 to 337 ± 0.6 Ma and 342 ± 1 to 334 ± 0.6 Ma, respectively, and are remarkably similar in age to an amphibolite-facies overprinting episode. Mica analyses from the Orlica Mountains also yield cooling ages between 338 ± 0.9 to 335 ± 0.5 Ma. Thermochronometry illustrates temporally disparate cooling histories but similar metamorphic evolutions between the Góry Sowie Block and the Orlica-Snieznik Complex. In both terranes, it took ~35 m.y. from the time of peak high-pressure conditions to residence in the upper crust, and possibly as little as 10 m.y. between high-pressure and mid-crustal supra-Barrovian events. These results in light of regional geochronology illustrate the rapid, localized and repetitious nature of eduction/exhumation of the Sudetic orogenic root including the eclogite and HP-granulite assemblages during protracted subduction.

INTRODUCTION

The Sudete Mountains are a mosaic of geologically diverse pre-Permian units within the northeastern Bohemian Massif, marking the eastern termination of the Variscides. The Sudetes are a narrow orogen, but are noted for their broadly contemporary blueschist, eclogite, and high-pressure (HP)-granulite metamorphic complexes in occurrence with ophiolitic sequences and igneous bodies of MORB-type affinities. The present spatial array of terranes in and around the corner of the Variscan belt reveals a disrupted orocline, dissected by dextral transpression induced through diachronous closure of the Rheic ocean. An apparent dissimilar metamorphic history for each of the crustal blocks clearly suggests the coexistence of several tectonostratigraphic terranes communicating during protracted convergence. The geodynamic welding of these terranes is a matter of some debate, and the unroofing and stabilization of a large part of this region is little investigated.

Of notable occurrence within the central Sudetes of the Polish-Czech border region are the presence of eclogite- and HP-granulite-facies assemblages that were preserved during the duration of Variscan assembly; timing and conditions of the descent and burial of these units are fairly well constrained (for example, O'Brien and

*Department of Geological Sciences, Ohio University, Athens, Ohio 45701, USA; schneidd@ohio.edu
**Department of Geology and Geophysics, University of Minnesota, Minneapolis, Minnesota 55455 USA
***Department of Geology, Geophysics and Environmental Protection, AGH-University of Science and Technology, Krakow, Poland

others, 1997; Bröcker and others, 1997). These once deep-seated assemblages are predominately enclosed as pods within supra-Barrovian (high-temperature/moderate-pressure) migmatites, orthogneisses, and amphibolites, which comprise the majority of the exposed terrane. However, the timing and mechanism of ascent (exhumation or eduction; Andersen and others, 1991) of these orogenic roots remains enigmatic. The simplest models that explain ultrahigh- and high-pressure (UHP and HP) exhumation invoke the coherent return of simple slabs initially driven by buoyancy gradients after descent of quartz-rich crustal material during subduction (for example, Chemenda and others, 1996; Walsh and Hacker, 2004). Because of diminishing body forces, isolated UHP and HP lenses stall and re-equilibrate in the lower crust. Eduction requires additional forces to bring the crustal slab to relatively shallow tectonic levels once the slab has exited the mantle and entered the overlying crustal stack. Some of this additional motion may be accomplished by subsequent thrusting due to continued convergence. Extensional collapse of an overthickened orogen may also contribute to exhumation through tectonic denudation via low-angle detachment surfaces. A third possible mechanism involves ductile extrusion of UHP and HP terranes between two bounding surfaces as these surfaces collapse together in a scissor fashion, in effect squeezing the terrane from deep to shallow tectonic levels through a combination of pure and simple shear (Vannay and Grasemann, 2001).

One or any combination of these processes can be considered as part of the eduction cycle, and during this ascent much of the surrounding lithospheric material undergoes supra-Barrovian metamorphism. Thus, a temporal relationship exists where the lower crust's peak metamorphic condition is coeval with a retrogressed path of the enveloped UHP and HP units. By constraining the cooling and exhumation history of the dominant migmatitic and gneissic crystalline basement exposed in the Sudetes, we attempt to evaluate the ascent mechanism of HP-bearing lower crustal rocks through the mid-crust.

Nearly all regional geochronologic investigations in the northern part of the Bohemian Massif have focused on terrane identification and division of the Cadomian-Variscan belt. Because of the plethora of crystallization dates produced, variable configurations of the different terranes across the massif have been a matter of lively discussion (for example, Matte and others, 1990; Oliver and others, 1993; Cymerman and Piasecki, 1994; Cymerman and others, 1997; Franke and Zelazniewicz, 2000; Aleksandrowski and Mazur, 2002) and we direct readers to those above references which are not further addressed here. Instead, it is the focus of this investigation to lend insight into, and to gain an understanding of, the post-assembly evolution of the eastern termination of the Varicides. Few published studies conducted within the Sudetes have acquired Variscan cooling and unroofing information (Steltenpohl and others, 1993; Maluski and others, 1995; Marheine and others, 2002); they provide useful age constraints for the detailed geological history of the orogen, but fail to address the timing and rate of tectonic processes. We therefore performed $^{40}Ar/^{39}Ar$ thermochronometry on two discrete terranes containing eclogite and HP-granulite assemblages within the central Sudetic belt to increase understanding of the exhumation of these rarely exposed, but fundamental, deep lithospheric components. Specifically, samples were collected and analyzed from the Orlica-Snieznik Complex (OSC) and the Góry Sowie Block (GSB), where existing petrologic, geochemical and higher-temperature geochronometric data on peak conditions provide a framework from which to construct an eduction model.

TECTONIC SETTING AND PREVIOUS GEOCHRONOLOGY

The Sudete Mountains consist of a collage of amalgamated Neoproterozoic to Lower Carboniferous terranes. Commonly correlated with the German segment of the Variscides, the Sudetes are thought to represent the southeastern-most extent of the

Saxo-Thuringian zone and the northeastern part of the Tepla-Barrandian unit (Bohemicum) (fig. 1; Crowley and others, 2002; Franke and Zelazniewicz, 2002). Basement metasedimentary and meta-igneous units within the Sudetes, which preserve centimeter to decimeter lenses of high-pressure rocks, have been intruded by a series of granitoid bodies during a complex tectonometamorphic history (Svoboda and Chaloupsky, 1966; Teisseyre, 1973; Zelazniewicz, 1997). Geochronometric investigations of the basement complex have provided constraints on two important geodynamic events prior to Variscan culmination: 1) an ~500 Ma granitic suite intrusion and 2) Caledonian tectonics (ca. 480 – 440 Ma) associated with the closure of the Iapetus/Tornquist ocean (Kröner and Hegner, 1998; Turniak and others, 2000). Reworking of the terranes continued with closure of the Rheic ocean, Eo-Variscan (ca. 400 – 360 Ma)

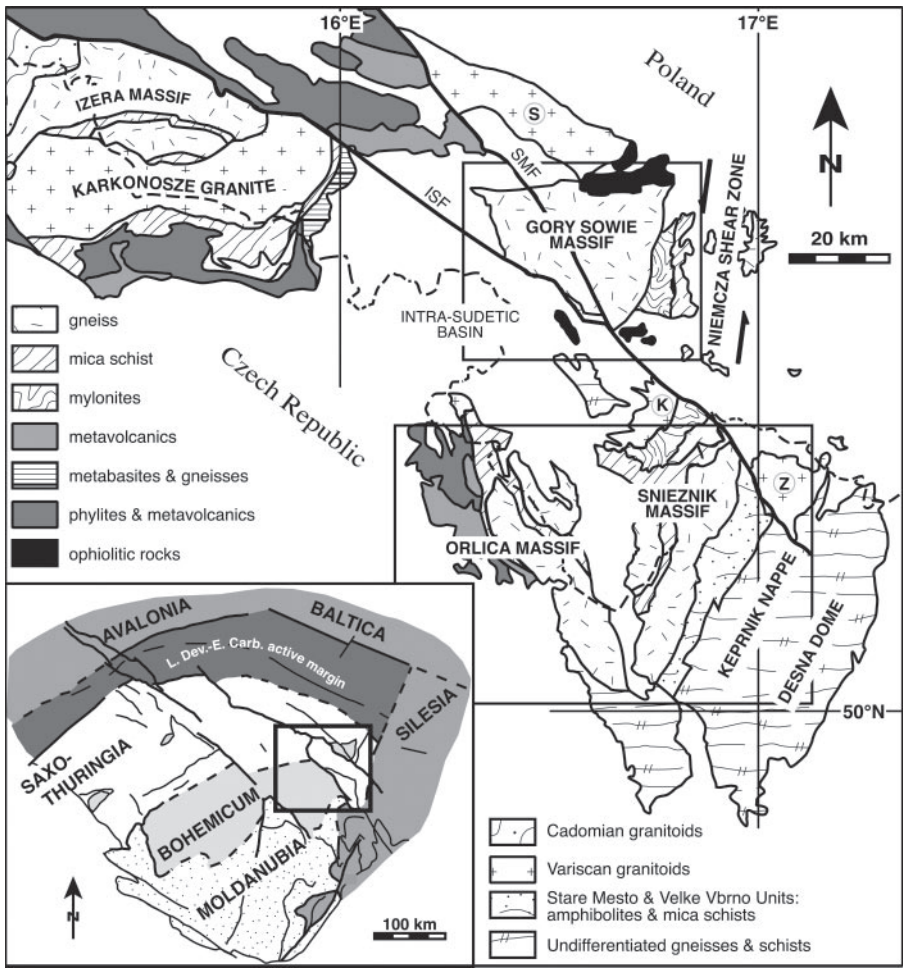

Fig. 1. Simplified geologic map of the Sudete Mountains (modified after Aleksandrowski and others, 1997). The two inset boxes show the location of the study areas (figs. 2 and 3) and unpatterned white region represents younger cover. Z: Zulova pluton. K: Klodzko-Zloty pluton. S: Strzegom-Sobotka pluton. ISF: Intra-Sudetic Fault. SMF: Sudetic Marginal Fault. INSET: Terrane map of the Bohemian Massif and adjacent zones (after Franke and Zelazniewicz, 2000). The box shows the general location of the Sudete Mountains in the northeast corner of the massif. Note the allochthonous nature of the Góry Sowie Block, which is separated by nearly 100 km from the rest of the Bohemicum terrane.

and Variscan (ca. 340 – 330 Ma) orogenic events, which included crustal thickening, metamorphic overprinting, and widespread contemporaneous magmatism (Turniak and others, 2000; Gordon and others, 2005). Tectonic structures abut to the east against the Silesia portion of the Brunia microcontinent, and are truncated by the NNE-trending Moldanubian Thrust, locally expressed in the Stare Mesto belt as the Nyznerov Thrust and containing significant dextral offset. In order to further constrain the exhumation history of the central Sudetes (fig. 1) samples were collected from two Variscan massifs, the Orlica-Snieznik Complex (OSC) and the allochthonous Góry Sowie Block (GSB), and an adjacent high-strain zone, the Niemcza shear zone. The following terrane descriptions and geochronology highlight the principal tectonothermal events; recently summarized geochronology is also reviewed in Marheine and others (2002).

Orlica-Snieznik Complex

In the central Sudetes, the Orlica-Snieznik complex (OSC) exposes a core of predominately amphibolite-facies (garnet- to locally kyanite-zone) granitoid gneisses, mylonites, migmatites and minor mica schists (fig. 2; Don and others, 1990; Steltenpohl and others, 1993; Lange and others, 2002). Eclogite and granulite assemblages are preserved as centimeter to decimeter boudins intercalated within the migmatitic orthogneisses. The deep crustal rocks attained peak metamorphic conditions within the coesite stability field of >27 kbar pressures and temperatures of ~700 to 800 °C, and subsequently underwent near isothermal decompression at conditions of 11 to 4 kbar and ~600 °C (Kryza and others, 1996; Bröcker and Klemd, 1996; Kozlowski and Bakun-Czubarow, 1997). More recently, Stípská and others (2004) disputed the thermobarmetric constraints of the UHP episode and report lower peak high-pressure conditions of 18 kbar at 900 °C. Structurally, the OSC lacks the hallmark characteristics

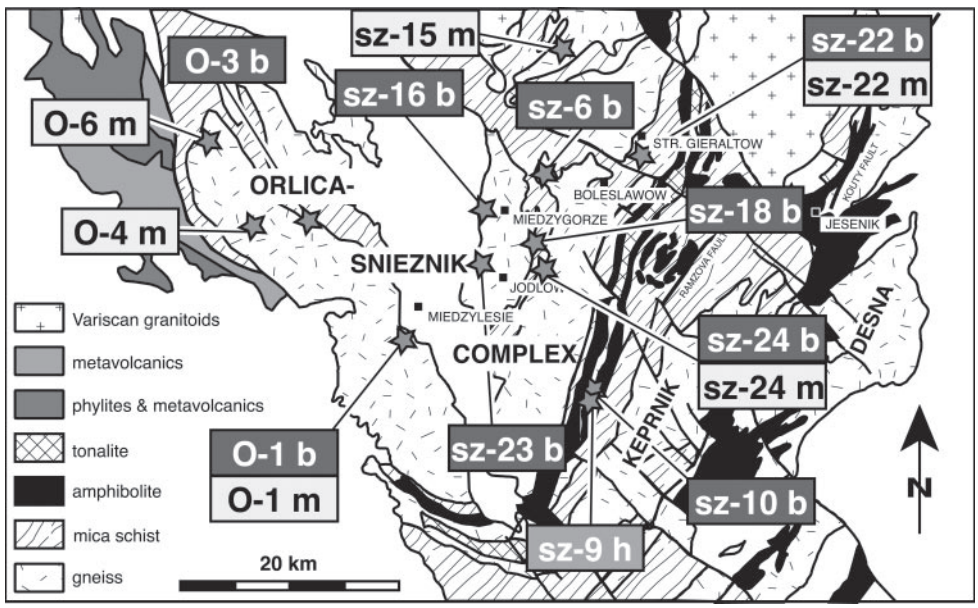

Fig. 2. Simplified geologic map of the Orlica-Snieznik Complex, showing main lithologic units, structural elements and sample locations (modified after Maluski and others, 1995). Primary high-pressure assemblages occur near Miedzygorze. Unpatterned white region represents younger cover. Sample labels include mineral analyzed: b: biotite; m: muscovite; h: hornblende.

of a gneiss dome, and instead preserves narrow subvertical ductile deformation zones surrounded by regions of dominantly subhorizontal fabrics, both fabric sets containing a gently plunging SSW mineral and magnetic lineation (Pressler and others, 2005a, 2005b). Notably, units containing high-pressure assemblages typically have a vertical fabric (Rychleby granulite belt and Miedzygorze belt) and still maintain the dominant subhorizontal lineation, but the cross-cutting relationship between the horizontal and vertical fabrics is ambiguous.

Flanked on the western side by greenschist-facies metasedimentary and metavolcanic rocks, the OSC is the western 'dome' in an east-west corridor of Variscan structures that include the OSC, Keprník and Desná domes, the latter two in the Jesenik Mountains. The NNE-trending Stare Mesto belt, a highly strained complex of intercalated lower-crustal and volcano-sedimentary rocks that is the hanging wall of the Moldanubian Thrust, separates the Snieznik and Jesenik Mountains. The evolution of these massifs has been attributed to extensional collapse resulting in core complexes (Steltenpohl and others, 1993; Cymerman, 1997) and/or Variscan dextral transpression producing a stacked nappe pile (for example, Aleksandrowski and Mazur, 2002). More recent structural and petrologic analyses suggest that the OSC is possibly a result of combined vertical extrusion and lateral flow during synconvergent exhumation (Stípská and others, 2004; Gordon and others, 2005; Pressler and others, 2005a,2005b).

The age of the supracrustal series enveloping Early Paleozoic igneous intrusions in the Orlica-Snieznik complex is hitherto poorly constrained at Neoproterozoic to Middle Cambrian (Borkowska and others, 1990; Gunia, 1990; Kröner and others, 2001). Based on Pb/Pb and U-Pb zircon ages on ortho- and paragneisses, remobilization of the crust occurred at ca. 500 Ma through emplacement of granitoid plutons (for example, Oliver and others, 1993; Kröner and others, 1994a; Kröner and others, 1994b; Turniak and others, 2000; Kröner and others, 2001). Combined Lu-Hf garnet geochronology and *in situ* trace element analyses constrain the time of peak (UHP?) metamorphism in the granulites at 387 ± 3 Ma (Szczepanski and others, 2004). Younger U-Pb zircon ages from orthogneisses and an omphacite-bearing granulite constrain the timing of Eo-Variscan HT-HP metamorphism to ca. 370 to 360 Ma in the Snieznik portion of the complex (Bröcker and others, 1997). Recent *in situ* Th-Pb monazite geochronometric data record an age of ca. 375 Ma also thought to represent the peak metamorphism in the Orlica Mountains (Gordon and others, 2005). In contrast, Brueckner and others (1991) reports Sm-Nd garnet-clinopyroxene-whole rock ages between 352 and 326 Ma for mafic granulite and eclogitic lenses from the high-pressure Zlote region of the northeastern OSC, which they interpreted as timing the HT-HP metamorphism. The combined Sm-Nd and U-Th-Pb data, albeit yielding a dispersed range of ages, suggest that ultrahigh- to high-pressure metamorphism may have locally lasted 30 m.y.; some of these results may equally be interpreted as the result of partially reset or mixed dates. In any case, eclogite and granulite of similar age are preserved in the Erzgebirge and Granulitgebirge of the Saxo-Thuringian zone of Germany, likely a record of subduction of continental crust (Franke and Stein, 2000).

Variscan events in the OSC region are revealed through several Pb, Sr, and Ar isotopic geochronologic investigations that constrain supra-Barrovian metamorphism and subsequent cooling through the Visean (Borkowska and others, 1990; Steltenpohl and others, 1993; Maluski and others, 1995; Bröcker and others, 1997; Turniak and others, 2000; Marheine and others, 2002; Stípská and others, 2004; Gordon and others, 2005). These 345 to 325 Ma dates are in marked contrast to the younger 310 to 300 Ma $^{40}Ar/^{39}Ar$ cooling ages reported for the Keprník and Desná domes of the Jesenik Mountains further to the east (Maluski and others, 1995), which belong to the footwall of the Moldanubian Thrust system within the Brunian/Silesian branch of the Variscan belt. Notably, no significant ultrahigh-pressure or ultrahigh-temperature assemblages

have been identified from this eastern footwall nappe structure. Widespread anatexis broadly associated with Variscan tectonics resulted in the emplacement of the Karkonosze, Klodzko, Strzegom-Sobotka, and Zulova plutons, significant undeformed granitoid bodies in the Sudetes (fig. 1). Although preliminary thermochronology tentatively records relatively rapid exhumation, and orogenic collapse has been suggested (compare, as early as Steltenpohl and others, 1993), unequivocal major normal-motion detachment structures have yet to be identified with in the Orlica or Snieznik Mountains.

Góry Sowie Block

The 650 km^2 Góry Sowie Block is a fault-bounded, triangular-shaped terrane preserving abundant migmatized gneisses and lesser amounts of serpentinites, amphibolites, and calc-silicate rocks (fig. 3). Within this amphibolite-facies matrix, centimeter to decimeter lenses of granulite are exposed and are usually accompanied by mantle-derived peridotites (Smulikowski and Bakun-Czubarow, 1969; Bakun-Czubarow, 1983; Zelazniewicz, 1985). The Sudetic Marginal Fault (SMF) divides the GSB into its mountainous western and poorly exposed low-lying eastern sections. The block is flanked on its western and northern sides by two sedimentary basins containing detritus from the GSB: the Intra-Sudetic Depression containing Visean and younger sediments, and the Famennian to Tournaisian deposits of the Swiebodzice Basin (Porebski, 1981, 1990). The detritus located in these basins corresponds with the

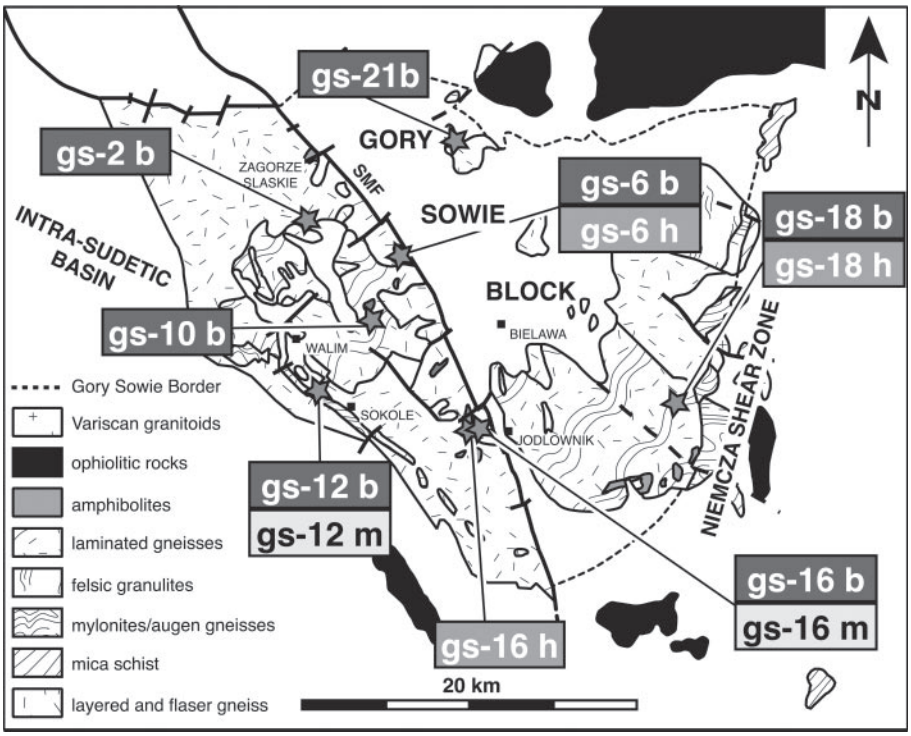

Fig. 3. Simplified geologic map of the Góry Sowie Block and Niemcza shear zone. The map shows the main lithologic units, structural elements and sample locations (modified after Bröcker and others, 1998). Primary high-pressure assemblages occur near Zagorze Slaskie. Unpatterned white region represents younger cover. SMF: Sudetic Marginal Fault. Sample labels include mineral analyzed: b: biotite; m: muscovite; h: hornblende.

mid-Visean clastic deposits that overstep the amphibolite-facies country rock of the GSB (Zakowa, 1963), and places stratigraphic constraints on the surface exposure of the massif during that period (320 – 300 Ma). The GSB is also bordered by numerous ophiolitic complexes (Sleza, Nowa Ruda, Braszowice and Szklary units), which have been dated at 420 +20/-2 Ma (U-Pb zircon age on gabbro; Oliver and others, 1993) and 400 +4/-3 Ma (U-Pb zircon on plagiogranite; Zelazniewicz and others, 1998; Dubinska and others, 2004), the latter date constraining only the minimum age of the igneous protolith. The difference in metamorphic grade and in age between the GSB and its flanking units has yielded an interpretation that the Góry Sowie is an allochthonous block thrust over the adjacent ophiolites (Cymerman, 1987; Bröcker and others, 1998). This is supported by gravimetric evidence suggesting the continuation of the gabbro and serpentine massif beneath the GSB (Znosko, 1981). Other interpretations include a klippe, an 'orogenic diapir' and/or a microcontinent (Kossmat, 1925, 1927; Jamrozik, 1981; Behr and others, 1982; Cwojdzinski, 1982; Oberc, 1991).

For the GSB, Pb/Pb single zircon evaporation ages from ortho- and paragneisses reveal granitoid emplacement into the Proterozoic basement during the Early Ordovician (Kröner and Hegner, 1998). Subsequent peak metamorphic conditions (900 – 1000 °C and 15 – 20+ kbar) were attained at ca. 400 Ma as revealed by O'Brien and others' (1997) U-Pb and Pb/Pb zircon ages of 402 ± 2 Ma and 399 ± 8 Ma for an HP-granulite unit. O'Brien and others' ages are concordant to an Sm-Nd garnet-clinopyroxene-whole-rock age of 402 ± 3 Ma for an adjacent garnet peridotite (Brueckner and others, 1996). The peak (ultrahigh and high) pressures and temperatures were overprinted by lesser conditions of 775 to 910 °C and 6.5 to 8.5 kbar (O'Brien and others, 1997). Furthermore, structural exhumation of the granulite and ultramafic sequences has been interpreted to be thermally connected and coeval with the prograde amphibolite-facies metamorphism of the surrounding host gneisses and migmatites (Zelazniewicz, 1987, 1990; Gordon and others, 2005). A significant high-temperature/moderate-pressure (supra-Barrovian) thermal event at ca. 380 Ma was revealed through conventional U-Pb monazite and xenotime ages on migmatites (van Breemen and others, 1988; Bröcker and others, 1998). Additionally, Timmermann and others (2000) reported U-Pb xenotime ages of 378 ± 2 Ma and 383 to 370 Ma for anatectic granite and pegmatite, respectively; prolific melting of the gneiss and migmatite sequences at this time suggests either increased heat flow or, more likely, isothermal decompression melting associated with unroofing events. Gordon and others (2005) obtained *in situ* ion microprobe Th-Pb monazite ages from two gneisses in the western part of the massif that suggest this may have been a protracted tectonothermal event lasting from ca. 385 to 370 Ma. Cessation of mid-crustal cooling for the western half of the GSB, probably associated with unroofing, likely occurred at ca. 360 Ma, constrained only by a few $^{40}Ar/^{39}Ar$ mica cooling ages from highly strained gneisses within the south-western massif (Marheine and others, 2002), as well as results from less robust methods (for example, Rb-Sr; Bröcker and others, 1998).

To the west and away from the GSB, the southern and eastern Karkonosze-Izera massif exposes blueschist-facies rocks, as well as MORB-type meta-igneous complexes; thermochronometry reveals initial cooling preserved at 360 Ma, which later witnessed a greenschist-facies overprinting event lasting until 320 Ma (Maluski and Patocka, 1997; Marheine and others, 2002). The Karkonosze terrane is interpreted as a pile of parautochthonous slices thrust to the northwest on the Saxo-Thuringian foreland (Schulmann and Gayer, 2000).

Truncating the eastern half of the block, the Niemcza-Kamieniec zone is, in part, a major NNE-SSW trending ductile shear zone (fig. 3). The deformed rocks are mainly of staurolite-zone mylonitized gneisses enveloping minor serpentinites and quartzogra-

phitic schists and are intruded by abundant granitoids (Mazur and Puziewicz, 1995; Józefiak, 2000). The shear zone was active with a sinistral displacement until the Early Carboniferous as revealed through U-Pb crystallization and $^{40}Ar/^{39}Ar$ cooling dates (Oliver and others, 1993; Steltenpohl and others, 1993; Cymerman, 1998). An age of 334 ± 2 Ma was revealed through Pb/Pb zircon dating of an anatectic granodiorite sample from the shear zone (Kröner and Hegner, 1998). Moreover, recently obtained geochronometric data indicates the NSZ was likely active over a period of approximately 100 m.y. (380 – 280 Ma; Gordon and others, 2005), which spans the entire tectonic evolution of the Sudetes.

$^{40}Ar/^{39}Ar$ thermochronology and analytical procedure

$^{40}Ar/^{39}Ar$ thermochronometry is an effective dating technique through which thermal histories of terranes are obtained in order to provide information on the timing and rate of geologic events. Typically amphibole, mica, and potassium-feldspar are the most utilized rock forming minerals for $^{40}Ar/^{39}Ar$ analysis because they are common in igneous and metamorphic rocks, and contain 5 to 10 weight percent of K^+. Moreover, these minerals are dated because of their high retention of argon under moderate closure temperatures. Hornblende is exceedingly retentive of radiogenic argon with a high closure temperature at moderate cooling rates of 500 ± 25 °C. Thus, the maximum age for cooling through the closure temperature for argon retention in hornblende is disclosed by the apparent age. Muscovite and white mica, which are stable over a wide range of metamorphic conditions, have a closure temperature for moderate cooling rates of 350 ± 25 °C, and the biotite $^{40}Ar/^{39}Ar$ age reflects the time of cooling below a closure temperature of 300 ± 25 °C, (McDougall and Harrison, 1999). For our study of the exhumation of the notable Orlica-Snieznik and Góry Sowie complexes, hornblende and mica were separated from metamorphic rocks for $^{40}Ar/^{39}Ar$ age spectrum analysis. Size fractions of >150 μm of the target minerals were obtained using standard crushing, heavy liquids, a Frantz magnetic separator, and careful handpicking to insure 99 percent purity. All samples were ultrasonically cleaned for five to ten minutes, rinsed in acetone, and dried at ~100 °C. Mineral separates were loaded into machined Al discs and irradiated with flux monitor Fish Canyon Tuff sanidine (27.84 Ma; Deino and Potts, 1990) for 100 hours in the L-67 position at the 2 MW Ford Reactor at the University of Michigan.

Isotopic analyses were conducted at New Mexico Tech using a MAP 215-50 mass spectrometer on line with automated all-metal extraction system. The flux monitor crystals were placed in a copper planchet within an ultrahigh vacuum argon extraction system and fused with a 10W Synrad CO_2 continuous laser. Evolved gases were purified for two minutes using a SAES GP-50 getter operated at ~450 °C. J-factors were determined to a precision of 0.1 percent (2σ) by analyzing a minimum of four single crystal aliquots from each of 3 to 4 radial positions around the irradiation sample trays. The unknown minerals were step-heated in a double-vacuum Mo resistance furnace; hornblende was heated for nine minutes and micas were heated for eight minutes. The gas was scrubbed of reactive species during heating with a SAES GP-50 getter for six to eight minutes at 450 °C. Following heating, the sample gas was further cleaned with another GP-50 for three minutes for micas and eight minutes for hornblende. Argon isotopic compositions for both the samples and monitors were determined using an electron multiplier with an overall sensitivity ranging from 2.66×10^{-16} moles/pA.

Extraction system and mass spectrometer blanks and backgrounds were measured numerous times throughout the course of the analyses. Typical blanks (including mass spectrometer backgrounds) were 1400, 18, 0.3, 2.7, and 4.8×10^{-17} moles at masses 40, 39, 38, 37, and 36, respectively, for furnace temperatures below 1300 °C. Correction factors for interfering nuclear reactions were determined using K-glass and CaF_2 and are as follows: $(^{40}Ar/^{39}Ar)_K = 0.0256 \pm 0.0015$; $(^{36}Ar/^{37}Ar)_{Ca} = 0.00027 \pm 0.00001$;

and $(^{39}Ar/^{37}Ar)_{Ca} = 0.00070 \pm 0.00005$. All errors are reported at the 2σ confidence level and the decay constants and isotopic abundance are those suggested by Steiger and Jaeger (1977). The reported plateau age is the inverse-variance-weighted mean of selected steps composed of contiguous increments representing >60 percent of gas released (and usually >70%) and represents the integrated ages calculated for the relatively flat portion of each age spectrum (using the concentration of ^{39}Ar to weight both individual ages and errors). This rationale assumes that the steps chosen do not contain excess ^{40}Ar and have not been highly affected by Ar recoil into alteration phases such as chlorite. The calculated plateau age uncertainties are relatively small because analytical precision in the age of each heating step is high. The K/Ca plots are determined from the Ca-derived ^{37}Ar and K-derived ^{39}Ar, of which the flattest parts of the age spectra generally correspond to relatively constant K/Ca values, whereas the younger apparent ages yield relatively high K/Ca values (Marcoline and others, 1999). The age spectra along with the K/Ca plots for the samples are presented in figure 4 and the analytical results are summarized in table 1 with isotopic details presented in the Appendix.

$^{40}Ar/^{39}Ar$ thermochronometric results

We sampled primarily the crystalline amphibolite-facies gneiss, schist, and amphibolite units from the central Sudete Mountains with a goal of constraining the timing of cooling, eduction and stabilization of the massifs. The cooling dates help constrain the timing and rate of exhumation of the basement country rock, along with the eclogite and HP-granulite lenses, through mid-crustal depths subsequent to supra-Barrovian metamorphism. A summary of lithologies, sample location and cooling age information is presented in table 1; Zahniser (ms, 2004) and Glascock (ms, 2004) provide further detailed location of samples selected for thermochronology, and their petrographic examination of samples demonstrate that the rocks ultimately chosen for analyses were the least altered and/or retrograded.

Orlica-Snieznik Complex

For the eastern (Snieznik) side of the complex (fig. 2), eleven mineral separates from nine rock samples were chosen for their mineral assemblage and mineral quality for $^{40}Ar/^{39}Ar$ dating. In addition, four gneisses and schists from the western (Orlica) side of the dome yielded five mineral separates available for analyses. It is the eastern portion that contains eclogite-bearing assemblages (near Miedzygorze) and the complex overall preserves a widespread garnet-zone amphibolite-facies signature (Glascock, ms, 2004). All of the rocks sampled are medium to coarse grained in texture and contain strained (sutured and undulatory) quartz. Garnet and plagioclase, when present, is poikilolitic; the garnet is often rotated and contains 'tails.' In total, sixteen mineral separates were chosen for analysis because of the abundance and/or quality of the hornblende, white mica, and biotite (fig. 4).

The nine samples from the Snieznik massif consist of six mica gneisses, two mica schists, and one amphibolite. A coarse-grained garnetiferous gneiss (sz-10A) collected from the southeastern area of the Snieznik massif, revealed a somewhat concordant spectrum for a biotite separate with the third through the eighth increments yielding a plateau age of 338.2 ± 0.5 Ma (MSWD: 3.78). A slightly (chlorite) retrogressed sample (sz-15) was collected from a well-foliated mica gneiss unit located in the northern area of the Snieznik massif and yielded a weakly saddle-shaped spectrum with a muscovite plateau age of 340.9 ± 0.5 Ma (MSWD: 1.28) over ~90 percent of the gas released. Analysis of biotite from a biotite-zone augen gneiss (sz-16) collected just west of Miedzygorze revealed a relatively flat spectrum with a plateau age of 333.9 ± 0.5 Ma (MSWD: 5.45) with ~98 percent of the gas, defined by the second through the eleventh increments. Another biotite separate (sz-18) was collected from a coarse-

grained garnet-zone mica gneiss near the same area, and the second through eleventh increments are concordant with a plateau age of 337.6 ± 0.6 Ma (MSWD: 11.93). Biotite from sample sz-23A was separated from a medium-grained garnet-mica gneiss located in the central western region of the Snieznik massif. The spectrum shape consists of a slightly chaotic display of increments yielding a plateau age of 341.6 ± 1.1 Ma (MSWD: 24.27) as defined by the second through twelfth increments. A sample of well-foliated mica gneiss (sz-24) was collected just southeast of sz-23A, and yielded a step-like shape of the spectrum, revealing a biotite plateau age of 340.9 ± 0.9 Ma (MSWD: 10.74), which comprised ~ 98 percent of the gas released. Analysis of a coexisting muscovite revealed older, early steps that decrease as the K/Ca ratio increases with 94 percent of the cumulative gas released defining a plateau age of 336.9 ± 0.5 Ma (MSWD: 0.87).

Biotite from a sample of strongly foliated garnet-mica schist (sz-6) was collected from the northeastern side of the Snieznik massif, in which the garnets appear to be rotated; the third through the tenth increments comprise ~70 percent of the gas with a plateau age of 334.2 ± 0.8 Ma (MSWD: 6.49). Coexisting mica separates were sampled from a garnet-mica schist (sz-22B) collected south of Stary Gieraltow in the northeastern region of the Snieznik massif (fig. 2). The biotite separate yielded concordant third through eighth increments with a plateau age of 339.1 ± 0.6 Ma (MSWD: 2.61), which comprises ~70 percent of the gas. The muscovite separate yielded a blocky-shaped spectrum with a similar plateau age of 334.9 ± 0.9 Ma (MSWD: 0.79), representing close to 100 percent of the gas released.

An amphibolite (sz-9) was collected from the southeastern side of the Snieznik massif in which the hornblende separate yielded an integrated age of 406 ± 3 Ma (fig. 4). However, three relatively concordant increments (F, G, and J) revealed an average weighted age of 391.1 ± 3.2 Ma (MSWD: 19). The chaotic nature of the spectrum is likely the result of hornblende contaminated with a fine-grained, relatively high-K non-retentive mineral (chlorite), and in thin section the amphibole is subhedral in appearance and intergrown with quartz. The variable amount of degassing of the two or more phases is represented by the complexity of the step-heating increments.

Mineral separates were also analyzed from the Orlica Mountains, which comprises the western portion of the dome complex (fig. 2). A biotite separate from a micaceous gneiss (O-1) yielded a relatively flat spectrum comprised of ten increments revealing a plateau age of 334.9 ± 0.4 Ma (MSWD: 4.92), which constitutes 96 percent cumulative gas released. In thin section, the medium grained rock also contains fragmented garnet. A muscovite separate was analyzed from the same sample (O-1) with a plateau age of 335.5 ± 0.8 Ma (MSWD: 0.72). A micaceous gneiss (O-4) from the west-central portion of the massif was sampled for white mica and revealed a spectrum that has a plateau age of 337.9 ± 0.7 Ma (MSWD: 3.3), with increments eight through thirteen representing ~80 percent of gas released. Analyses of biotite from a mica schist (O-3) from the east-central side of the Orlica massif yielded a slightly dome-shape spectrum, characterized by the second through tenth increments with a plateau age of 338.2 ± 0.9 Ma (MSWD: 11.18). Sample O-6 is a muscovite separate from a coarse grained mica schist with a markedly younger integrated age of 311.9 ± 0.6 Ma in which increments eight through fifteen represent ~82 percent of gas released and a plateau age of 314.4 ± 0.8 Ma (MSWD: 3.63).

Góry Sowie Block

Incremental heating experiments were performed on twelve samples from five localities across the Góry Sowie Block (fig. 3; table 1), a predominantly relic granulite terrane. Most of the quartzofeldspathic assemblages preserve strain textures as undulose, polygonal and sutured quartz, and some rotation of the garnet (Zahniser, ms, 2004). Fibrous sillimanite is common in the northern massif, occurring along foliation

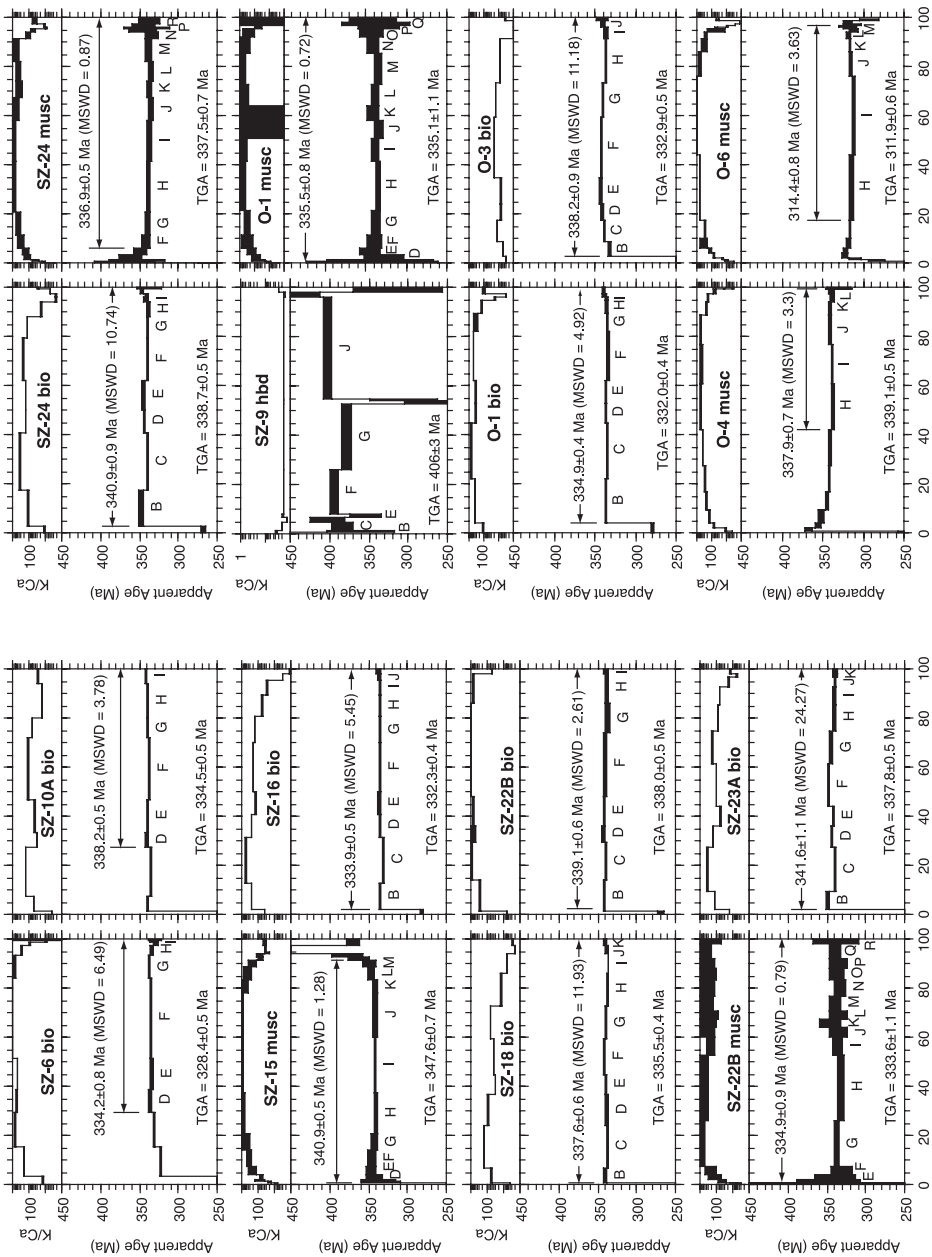

Fig. 4. ^{40}Ar/^{39}Ar age spectra and corresponding K/Ca ratios for Orlica (O-), Snieznik (sz-), and Góry Sowie (gs-) massifs. Lettered increments correspond to table in Appendix, and are only listed for the steps that define the plateau age. TGA: total-gas age.

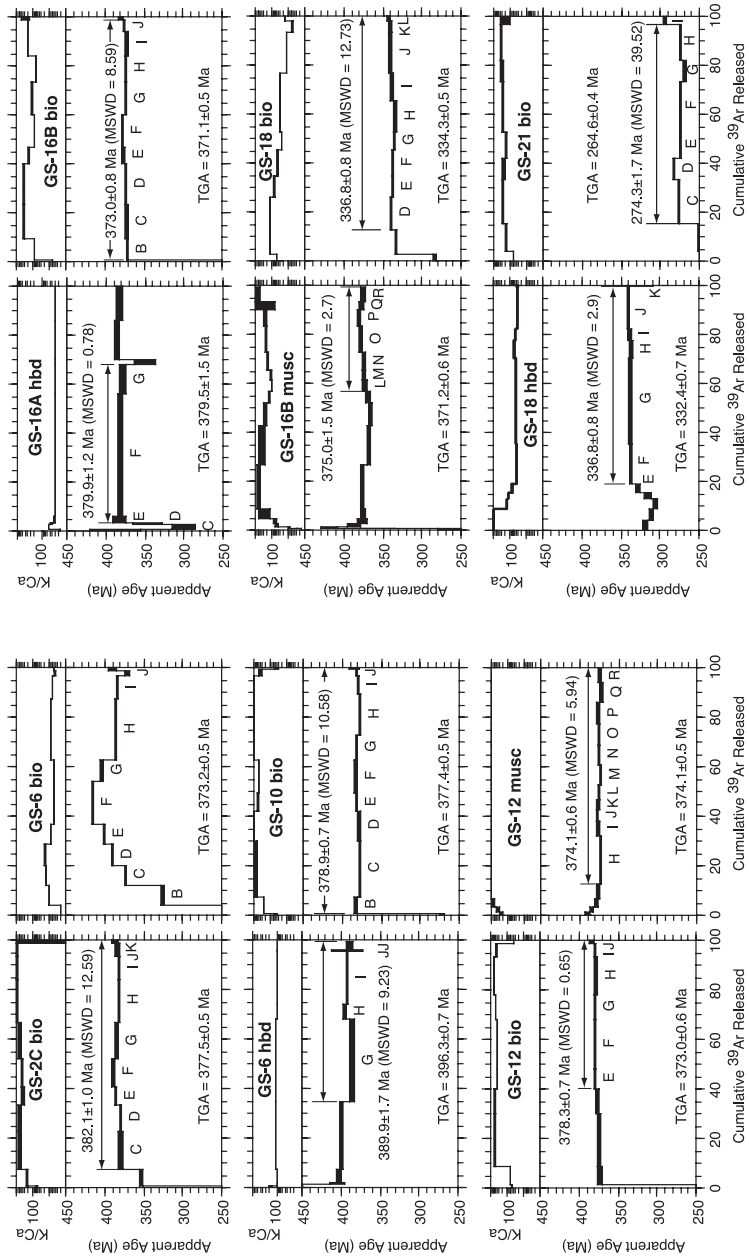

Fig. 4. (*continued*)

TABLE 1

Summary of sample lithology, location, and $^{40}Ar/^{39}Ar$ cooling ages from NE Bohemian Massif

Orlica-Snieznik Complex							
sample	**lithology**	**location**		**TGA (Ma)***	**Tp (Ma)***	**MSWD**	**% ^{39}Ar**
O-1	garnet gneiss	Lichkov	bio	332.0 ± 0.4	334.9 ± 0.4	4.92	96
O-1	garnet gneiss	Lichkov	musc	335.1 ± 1.1	335.5 ± 0.8	0.72	99
O-3	coarse mica shist	Rudawa	bio	332.9 ± 0.5	338.2 ± 0.9	11.18	90
O-4	gneiss	Ricky	musc	339.1 ± 0.5	337.9 ± 0.7	3.30	79
O-6	coarse mica shist	Zieleniec	musc	311.9 ± 0.6	314.4 ± 0.8	3.63	82
sz-6	coarse mica shist	Sienna	bio	328.4 ± 0.5	334.2 ± 0.8	6.49	71
sz-9	foliated amphibolite	Vjtiskov	hbd	406.2 ± 2.5	N/A	-	-
sz-10A	garnet gneiss	Vjtiskov	bio	334.5 ± 0.5	338.2 ± 0.5	3.78	72
sz-15	micaceous gneiss	Radochow	musc	347.6 ± 0.7	340.9 ± 0.5	1.28	92
sz-16	augen gneiss	Radochow	bio	332.3 ± 0.4	333.9 ± 0.5	5.45	98
sz-18	micaceous gneiss	Miedzygorze	bio	335.5 ± 0.4	337.6 ± 0.6	11.93	91
sz-22B	coarse mica shist	Nova Gieraltow	bio	338.0 ± 0.5	339.1 ± 0.6	2.61	70
sz-22B	coarse mica shist	Nova Gieraltow	musc	333.6 ± 1.1	334.9 ± 0.9	0.79	98
sz-23A	micaceous gneiss	Weis	bio	337.8 ± 0.5	341.6 ± 1.1	24.47	91
sz-24	gneiss	Yelka	bio	338.7 ± 0.5	340.9 ± 0.9	10.74	98
sz-24	gneiss	Yelka	musc	337.5 ± 0.7	336.9 ± 0.5	0.87	94
Góry Sowie Block							
sample	**lithology**	**location**		**TGA (Ma)***	**Tp (Ma)***	**MSWD**	**% ^{39}Ar**
gs-2C	micaceous gneiss	Byrtryzyckie Lake	bio	377.5 ± 0.5	382.1 ± 1	12.59	90
gs-6	amphibolite	Podole	bio	373.2 ± 0.5	N/A	-	-
gs-6	amphibolite	Podole	hbd	396.4 ± 0.7	389.9 ± 1.7	9.23	65
gs-10	micaceous gneiss	Potoczek	bio	377.4 ± 0.5	378.9 ± 0.7	10.58	99
gs-12	micaceous gneiss	Sokolec	bio	373.0 ± 0.6	378.3 ± 0.7	0.65	60
gs-12	micaceous gneiss	Sokolec	musc	374.1 ± 0.5	374.1 ± 0.7	5.94	85
gs-16A	amphibolite	Jodlownik	hbd	379.5 ± 1.5	379.9 ± 1.3	0.78	70
gs-16B	gneiss	Jodlownik	bio	371.1 ± 0.5	372.4 ± 0.8	12.60	99
gs-16B	gneiss	Jodlownik	musc	371.2 ± 0.6	375.0 ± 1.5	2.70	57
gs-18	amphibolite	Bradziszow	bio	334.3 ± 0.5	336.8 ± 0.9	12.73	85
gs-18	amphibolite	Bradziszow	hbd	332.4 ± 0.7	336.8 ± 0.8	2.87	85
gs-21	micaceous gneiss	Grodziszcze	bio	264.6 ± 0.4	274.3 ± 1.7	39.52	85

*TGA = integrated age; Tp = plateau age.

planes and occasionally replacing kyanite or garnet. Of the twelve analyzed samples, eleven returned well-defined plateau ages (fig. 4).

Four mineral separates were analyzed from a northern transect, the highest grade portion of the massif. Sample GS-2C is a well-foliated upper sillimanite-zone micaceous gneiss adjacent to amphibolite and granulite lenses, and contains kyanite inclusions within garnet. Incremental heating of biotite resulted in the first two increments demonstrating a gradual increase in age from 132 Ma to 352 Ma before reaching a well-defined plateau of 382.1 ± 1.0 Ma (MSWD: 12.59) over the final nine increments (90% of the total gas).

Sample GS-6 contained co-existing coarse biotite and hornblende from a nonfoliated garnet-bearing amphibolite within the upper garnet-zone. Analysis of biotite failed to produce a well-defined plateau over eleven increments, yielding a total gas age of 373.2 ± 0.5 Ma, although increments eight and nine produced a preferred age of 383.0 ± 10 Ma (MSWD: 2.80) constituting 35 percent of the total gas. Investigation of the hornblende revealed initially old ages (six increments) gradually decreasing from

405 Ma (increments three and four) to 395 Ma (increments five and six). The final six heating steps resulted in a plateau age of 389.9 ± 1.7 Ma (MSWD: 9.23) constituting 65 percent of the total gas released, slightly older than the biotite cooling age.

From the north-central massif, east across the SMF (fig. 3), biotite was analyzed from sample GS-21, an amphibolite-facies micaceous gneiss that contains small garnet. An age plateau exists for increments three through ten (85% of the total gas) and yielded an age of 274.3 ± 1.7 Ma (MSWD: 39.52), albeit with an extremely high MSWD. It is important to note that this sample contained strongly retrogressed garnet and serecite alteration of plagioclase that forms about 25 percent of the mode, suggesting a suspect isotopic date.

Three separates were selected for thermochronology from the central portion of the massif. Sample GS-10, a sillimanite-garnet gneiss of the upper sillimanite-zone, was processed for biotite analysis, which occurred as large, decussate tabular minerals. Ten of the eleven heating increments (99% of the total gas) produced an age plateau of 378.9 ± 0.8 Ma (MSWD: 10.58). Co-existing biotite and muscovite were analyzed from GS-12, a schistostic gneiss of the upper garnet-zone. Analysis of biotite revealed a fairly uniform age distribution of increments, though only increments five through nine contributed to a plateau age of 378.3 ± 0.7 Ma (MSWD: 0.65) with 60 percent of the total gas released. Muscovite analysis was conducted over sixteen heating increments with the first five increments showing a gradual decrease in age from 388 Ma to a plateau age of 374.2 ± 0.7 Ma (MSWD: 5.94) comprising 85 percent of the total gas.

The final five samples were collected within the southern GSB. Samples GS-16A and –16B were collected from two localities, roughly 50 m apart. Hornblende was separated from location A (a coarse-grained foliated garnet amphibolite lens), and co-existing muscovite and biotite from location B (a garnet gneiss containing sparse sillimanite). Analysis of GS-16A hornblende yielded a plateau age of 379.9 ± 1.3 (MSWD: 0.78) for increments five through seven with over 65 percent of the total gas contributing. Increment eight shows a markedly younger age, thus excluding the remaining heating increments from the plateau age. Incremental heating of muscovite from GS-16B, a garnetiferous gneiss in the lower sillimanite-zone, yielded initially older ages before attaining an age of 375.0 ± 1.5 Ma (MSWD: 2.70) for increments twelve through eighteen with 55 percent of the total gas contributing. While failing to meet the defined criteria of a plateau age that is 60 percent of the total gas released, we believe that this date nonetheless represents an accurate age of cooling. Biotite from sample GS-16B, in concordance with the muscovite age, yielded a uniform plateau age of 372.4 ± 0.8 (MSWD: 12.60) with approximately 99 percent of the total gas contribution.

Sample GS-18, a garnet-zone foliated amphibolite located adjacent to the Niemcza shear zone in the eastern GSB (fig. 3), was sampled for both biotite and hornblende (fig. 4). The rock is fine to medium grained and contains leucosomal boudins along foliation planes. Incremental heating of the hornblende revealed a gradual increase in age over the first five steps before reaching a plateau age of 336.8 ± 0.8 Ma (MSWD: 2.87) over the remaining six steps (85% of the total gas). Analysis of biotite also produced a gradual increase in ages before attaining an identical plateau age of 336.8 ± 0.9 Ma (MSWD: 12.73) with 85 percent of the total gas released.

DISCUSSION AND IMPLICATIONS

The Sudetes are a complex mosaic of peri-Gondwanan crustal fragments and arc terranes that are considered to be members of the Saxo-Thuringian and Moldanubian zones (Matte and others, 1990). Its components are welded together by (now closed) intervening narrow basins and seaways that resulted from a series of mutual collisions as well as collisions with Baltica (±Avalonia) culminating in the Variscan orogeny. Our thermochronometric investigation of the West Sudetes coupled with existing geochro-

nometric constraints on the adjacent metamorphic massifs directly to the west (Karkonosze) and to the east (Jesenik) have revealed two fundamental observations for the northeastern Bohemian Massif (fig. 5): i) the rapid nature of cooling and probable exhumation of, at least, the Orlica-Snieznik and Góry Sowie massifs and, ii) that timing constraints on cooling are remarkably consistent within discrete crustal domains, but markedly variable between adjoining terranes. Disparate and discrete thermal histories of adjoining crustal blocks is easy to envisage: multiple subduction/eduction events should not be surprising if the Iapetus and Rheic oceans were as littered with arcs, microcontinents, and oceanic plateaus as the southwestern Pacific ocean is today. Furthermore, the geodynamic complexities associated with corner effects of the Bohemian Massif in the region during convergence have produced a significant conservation of displacement in an attempt to accommodate the non-linear shape of the orogenic zone. First order observations suggest significant syn- to post-metamorphic crustal shuffling within the Sudetic region likely in response to these corner effects and orogen-normal lateral displacements. Following a revised geologic summary of the Sudetes through the Variscan, we invoke a model that we feel simplistically clarifies the sequence of tectonic events preserved in the orogen.

The final closure of the Paleozoic circum-Sudetic seaways by oceanic lithospheric subduction was likely associated with ultrahigh-pressure metamorphism. The earliest high-pressure, high-temperature event (15 – 20 kbar, 1000 °C) occurred at 400 Ma, as

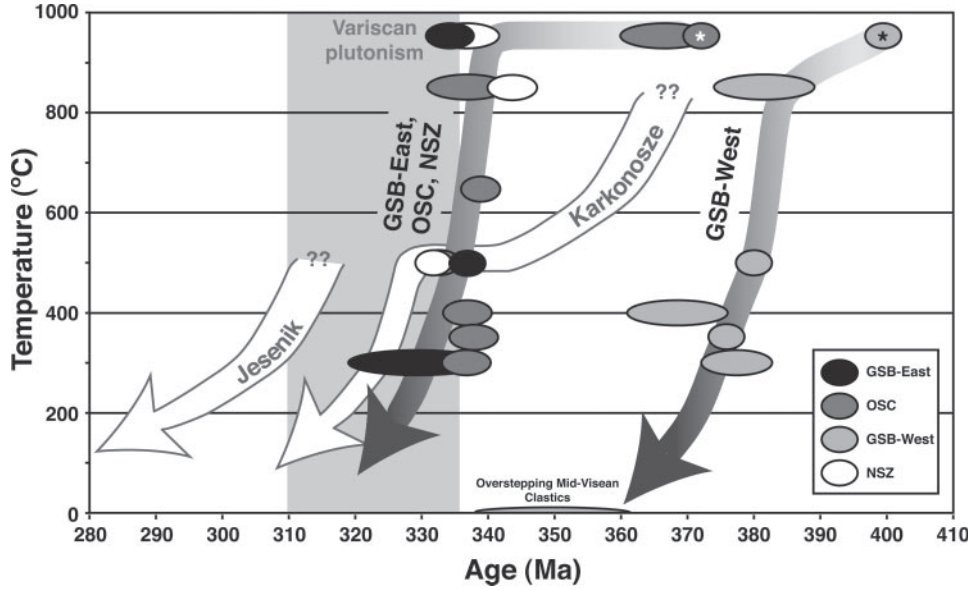

Fig. 5. Temperature-time evolution of the central Sudete Mountains based on published geochronometry and the results of this study. Note the coincident cooling histories for the OSC, Niemcza shear zone (NSZ) and eastern half of the GSB relative to the older cooling path for the western half of the GSB. Cooling paths for Karkonosze and Jesenik terranes are only schematically portrayed. Ellipses represent the age bracket constrained at closure temperatures of specific geochronometers: 1000 °C: U-Pb zircon and Sm-Nd mineral pairs, 850 °C: U-Pb and Th-Pb monazite and xenotime, 500 °C: $^{40}Ar/^{39}Ar$ hornblende, 400 °C: Rb-Sr biotite, 350 °C: $^{40}Ar/^{39}Ar$ muscovite, 300 °C: $^{40}Ar/^{39}Ar$ biotite. A single ellipse may contain more than one date; longer ellipses contain a range of dates. Asterisk ellipses are HP or UHP dates. Data from: van Breemen and others, 1988; Borkowska and others, 1990; Brueckner and others, 1991; Oliver and others, 1993; Steltenpohl and others, 1993; Maluski and others, 1995; Brueckner and others, 1996; O'Brien and others, 1997; Bröcker and others, 1997; Bröcker and others, 1998; Kröner and Hegner, 1998; Turniak and others, 2000; Timmermann and others, 2000; Marheine and others, 2002; Stípská and others, 2004; Gordon and others, 2005; this study.

constrained by ages on felsic granulite and garnet peridotite of the Góry Sowie Block (O'Brien and others, 1997; Bröcker and others, 1997). These rocks, as well as the majority of the GSB crystalline basement, underwent subsequent supra-Barrovian metamorphism that instigated widespread anatexis and migmatization at conditions of >700 °C and 4 to 5 kbar across the GSB beginning at 390 Ma (van Breeman and others, 1988; Bröcker and others, 1998; Timmerman and others, 2000; Gordon and others, 2005). Our data show for the mountainous western portion of the GSB, $^{40}Ar/^{39}Ar$ hornblende plateau ages are 390 to 380 Ma and mica plateau ages are 382 to 372 Ma, illustrating a slight north to south younging trend. Muscovite $^{40}Ar/^{39}Ar$ analyses from the southwest margin of the massif further support this trend with ages of 360 Ma (Marheine and others, 2002). The age trend is also associated with a distinct metamorphic relationship in the western block: metamorphic grade is granulite-facies in the north, progressively decreasing to biotite-zone amphibolite-facies toward the south (Zahniser, ms, 2004). Our thermochronometric data coupled with published higher-temperature metamorphic ages reveals collapsed chronologies between >700 °C and 300 °C (fig. 5), signaling rapid cooling following supra-Barrovian conditions and probably rapid exhumation from lower crustal levels. While not unequivocal, rapid cooling is likely related to rapid unroofing, since the provenance of conglomerate sequences in the adjacent and overlying Late Devonian sedimentary basins has been traced to the Góry Sowie (Zakowa, 1963; Porebski, 1981, 1990).

Notably within the GSB, the eastern portion of the massif as well as the adjacent Niemcza shear zone remained thermally elevated or were reheated during the mid-Visean: published metamorphic ages and our $^{40}Ar/^{39}Ar$ cooling dates from this region suggest continued tectonothermal activity within and along the shear zone (fig. 5). Ion microprobe *in situ* Th-Pb monazite analyses from two tectonite samples of the Niemcza zone reveal a range of dates from 380 to 280 Ma (Gordon and others, 2005), illustrating the long-lived deformation within this shear zone. One sample we collected within the Niemcza shear zone yielded concordant coexisting hornblende and biotite plateau ages of 337 Ma, similar to the cooling ages of the Orlica-Snieznik complex to the south. Syn- and post-tectonic granitoids within the Niemcza zone have been dated via Pb/Pb zircon analyses at ca. 334 Ma (Kröner and Hegner, 1998), and preliminary single crystal $^{40}Ar/^{39}Ar$ total fusion ages from mylonites show a range of ages between 337 ± 13 and 319 ± 17 Ma (Oliver and Kelley, 1993). A retrogressed sample from the eastern GSB resulted in a much younger biotite cooling age of 274 Ma reported here. In general, crystallization and cooling ages for the Niemcza zone along the eastern margin of the GSB are in accord, and indicate a significantly younger thermal evolution with respect to the western Góry Sowie.

In marked contrast to the western GSB, cooling ages from amphibolites and gneisses of the Orlica and Snieznik Mountains are nominally 40 m.y. younger (fig. 5). The majority of the age spectra reported in this investigation from amphibolite-facies units across the massif were similar in appearance and yielded strikingly consistent cooling ages with the exception of the one amphibole sample. Biotite analyses from the mica gneisses and schists of the OSC yielded $^{40}Ar/^{39}Ar$ plateau ages of 342 to 333 Ma, with a weighted age for all samples of 336.7 ± 1.9 Ma (MSWD: 17). While there is a 10 m.y. spread in cooling dates, all the spectra appear to be well behaved but lack any strong geographic or structural trend. Muscovite also yielded a similar range of $^{40}Ar/^{39}Ar$ plateau ages between 341 to 334 Ma, with a weighted age of 337.6 ± 3.1 Ma (MSWD: 18), plus one sample dated at 314.4 ± 0.8 Ma. A hornblende from the southeastern side of the Snieznik massif yielded an integrated (total gas) age of ca. 400 Ma; since no plateau was achieved, its reliability is inherently dubious. Our ages are comparable to the preliminary ages reported in Maluski and others (1995) for migmatites and amphibolites of the eastern Snieznik Mountains; they report horn-

blende and biotite $^{40}Ar/^{39}Ar$ ages of 336 to 328 Ma, and a muscovite age of 313 Ma. Massif-wide cooling through the 400 – 300 °C isotherms at 340 to 330 Ma is remarkably concordant with reported U-Pb zircon and Th-Pb monazite dates from the massif, which constrain higher temperature (locally granulite-facies) metamorphic events. The striking cluster of published geochronometric data and newly reported data that yield Visean ages across a range of closure temperatures (fig. 5), coupled with the supra-Barrovian overprint signature (650 °C at 4 – 11 kbar), is indeed indicative of rapid eduction from the lower lithosphere through distinct amphibolite-facies conditions followed by rapid cooling.

In general, the Famennian to Visean denudation of the western GSB was coeval with significant tectonothermal activity in the surrounding Sudetic terranes related to microcontinent collision that thrust the metamorphic complexes over the foreland (Maluski and Patocka, 1997; Cymerman and others, 1997). We have already demonstrated the diachroneity between the GSB and OSC with our own results; published thermochronometric results reported from the Jesenik and Karkonosze Mountains suggest those terranes appear to have also suffered relatively punctuated thermal evolutions (fig. 5). Fifty kilometers to the west of the GSB and across the Intra-Sudetic fault, Eo-Variscan subduction-related blueschist-facies metamorphism in the Rychory Mountains of the Karkonosze complex is constrained to $<$500 °C and 7 to 10 kbar (Patocka and others, 1996) and cessation of that metamorphism is dated at 365 Ma (fig. 5; Maluski and Patocka, 1997). The blueschist-facies metamorphism was followed by tectonic exhumation under upper greenschist-facies conditions at ca. 345 Ma during Variscan compression (Maluski and Patocka, 1997; Marheine and others, 2002). Recall, the OSC shares a similar history: eclogite-facies metamorphism at 370 to 360 Ma likely dates the ultrahigh-pressure conditions of 700 to 800 °C and $>$27 kbar (Bröcker and Klemd, 1996) and, as our $^{40}Ar/^{39}Ar$ data indicate, similar Visean cooling.

Directly east from the OSC across the Stare Mesto Belt, an expression of the Moldanubian Thrust, the Desná and Keprník domes of the Jesenik Mountains preserve even younger $^{40}Ar/^{39}Ar$ cooling ages of 315 to 282 Ma in amphibolite-facies rocks (Maluski and others, 1995). Cooling ages reported from high-pressure/low-temperature assemblages and surrounding variably deformed mylonites along the southeastern margin of the Karkonosze-Izera Massif to the west are primarily 330 to 315 Ma and date a greenschist-facies overprinting episode of blueschist-facies assemblages (Marheine and others, 2002). The younger cooling ages from these regions (fig. 5) suggest either prolonged burial at mid-crustal levels before slow unroofing, or localized reheating (and isotopic resetting) due to post-Variscan plutonism.

We acknowledge that our thermochronometric study only constrains the latter stages of any exhumation model, but our data in concert with higher temperature geochronology allow us to illustrate the rapid, localized and repetitious nature of eduction during protracted subduction. In both the GSB and OSC, it took ~35 m.y. from the time of peak high-pressure conditions to residence in the upper crust, and possibly as little as 10 m.y. between high-pressure and mid-crustal supra-Barrovian events. Furthermore the proximity of these terranes in light of their incongruent histories is quite striking: as the GSB was already quietly eroding away near the surface, the OSD was undergoing its own high-pressure event, possibly as close as 60 km away. If the GSB is indeed allochthonous (Cymerman, 1987; Bröcker and others, 1998), this is as equally impressive, as the eduction and the thrusting transport would have had to occur and cease within a similar time span. Considering the Jesenik and blueschist-bearing Karkonosze massifs in this already complicated picture, the Sudetes contain several punctuated eduction events during Variscan collision.

There is still clearly much work to do on the exhumation history of the Sudetes, but the emerging data appear to suggest that protracted subduction with multiple

episodes of eduction are required for the evolution of the orogen. We envisage more or less identical eduction histories commencing at 400 Ma and again at 370 Ma for the GSB and OSC, respectively, through a process termed dunk tectonics (Brueckner and van Roermund, 2004). After descent of quartz-rich crustal material during subduction, slab breakoff and buoyancy gradients drive the early eduction process. Initial ascent of the high-pressure rock was arrested in the lower or middle crust, where the mass of continental material would have ponded and undergone subsequent supra-Barrovian metamorphism. Preservation of (ultra-?) high-pressure assemblages indicate that the Bohemian rocks did not long remain in the lower crust, but were in fact exhumed before the peak metamorphic record could be completely erased. The widespread supra-Barrovian event during decompression triggered partial melting and extensive collapse of the thickened crust, facilitating a positive feedback between migmatization and rapid exhumation. Further evidence of widespread melting and segregation is in the form of the voluminous Variscan granitoids in the region (Klodzko, Karkonosze) that likely further thermally weakened the crust. The partially melted mid-crustal system would have allowed a fast upward migration of low-resistance material carrying small, resistant pods of eclogite and granulite. A process such we have outlined above would have repeated two or possibly three times over the span of the Variscan subduction and orogeny to result in the mosaic of terranes now present in northeastern Bohemia.

Due to a paucity of published structural studies focused on the Sudetes, the precise mechanism of eduction is unknown, but purported normal-motion detachment structures are ambiguously described in the literature (for example, Steltenpohl and others, 1993; Cymerman, 1997). Based on the geochronology, we can state eduction would have occurred during Variscan collision and not during post-orogenic collapse. Moreover, other structural data that is available from the GSB and OSC does indicate a further conundrum: eduction requires sub-vertical transport of material through the crust, however shallowly plunging N-S stretching lineation dominant the crystalline fabric, which can be attributed to pervasive lateral flow. Therefore, we speculate the subhorizontal fabrics and gently plunging lineations formed in the weak mid-crust below more rigid upper crustal blocks. Upon reaching the crustal high-strength lid and cessation of rapid vertical eduction, the ductile mass of continental material laterally overturned, horizontally spread and quickly cooled, locally preserving high-pressure relicts in sub-vertical fabrics that represent deeper structural levels. Further research documenting the structural architecture of the Sudetes is necessary to further resolve the eduction and exhumation mechanisms.

CONCLUSION

The Sudete Mountains of Poland and the Czech Republic contain all the hallmarks of an ancient suture zone: ophiolite sequences, blueschist-, eclogite- and granulite-facies rocks, and a complex lithotectonic character. Initial convergence occurred during the Cadomian orogeny, but the indelible geologic signature preserves Variscan activity, and notably discrete crustal blocks, now in proximity to one another, were at dramatically different depths during the Mid- to Late-Devonian. A temporally disparate but similar metamorphic evolution of the Góry Sowie Block occurring between 400 Ma and 360 Ma and the Orlica-Snieznik Complex occurring between 370 Ma and 330 Ma suggest recurring eduction during protracted subduction. Preliminary geochronologic investigations on the Karkonosze and Jesenik terranes further suggest somewhat comparable, yet diachronous episodes. Recently termed dunk tectonics by Brueckner and van Roermund (2004) for a similar scenario in the Scandinavian Caledonides, this exhumation style may be more widespread but little recognized than previously documented. The rapid and repetitious nature of this process during long-lived convergence may represent an effective mechanism to exhume and preserve deep crustal material in orogenic belts.

ACKNOWLEDGMENTS

This research was supported by grants from the US National Research Council (DAS) and Ohio University, and represents the results of MS thesis work conducted by SJZ and JMG. We thank Matt Heizler at New Mexico Tech for helping with the Ar-Ar thermochronometric analyses. Discussions and manuscript comments from D. Holm, L. Webb, H. Brueckner, and S. Mazur helped improve the details and flow of this paper.

References

Aleksandrowski, P., and Mazur, S., 2002, Collage tectonics in the northeasternmost part of the Variscan Belt: the Sudetes, Bohemian Massif, *in* Winchester, J. A., Pharaoh, T. C., and Verniers, J., editors, Palaeozoic Amalgamation of Central Europe: London, Geological Society Special Publication, v. 201, p. 237–278.

Andersen, T., Jamtveit, B., Dewey, J., and Swensson, E., 1991, Subduction and eduction of continental crust: Major mechanisms during continent-continent collision and orogenic extensional collapse, a model based on the southern Norwegian Caledonides: Terra Nova, v. 3, p. 303–310.

Bakun-Czubarow, N., 1983, Mineral chemistry of garnet lherzolites from the Sudetes, southwest Poland: Carnegie Institution of Washington, Yearbook, 82, p. 326–343.

Behr, H. J., Engel, W., and Franke, W., 1982, Variscan wildflysch and nappe tectonics in the Saxothuringian Zone (northeast Bavaria, West Germany): American Journal of Science, v. 282, p. 1438–1470.

Borkowska, M., Choukroune, P., Hameurt, J., and Martineau, F., 1990, A geochemical investigation of the age, significance, and structural evolution of the Caledonian-Variscan granite-gneisses of the Snieznik metamorphic area, central Sudetes, Poland: Geologia Sudetica, v. 25, p. 1–27.

Bröcker, M., and Klemd, R., 1996, Ultrahigh-pressure metamorphism in the Snieznik Mountains (Sudetes, Poland): P-T constraints and geological implications: The Journal of Geology, v. 104, p. 417–433.

Bröcker, M., Cosca, M., and Klemd, R., 1997, Geochronologie von Eklogiten und assoziierten Nebengesteinen des Orlica-Snieznik Kristallins (Sudeten, Poland): Ergebnisse von U-Pb, Sm-Nd, Rb-Sr und Ar-Ar Untersuchungen: Terra Nostra, v. 97/5, p. 29–30.

Bröcker, M., Zelazniewicz, A., and Enders, M., 1998, Rb-Sr and U-Pb geochronology of migmatitic gneisses from the Góry Sowie (West Sudetes, Poland): the importance of Mid-Late Devonian metamorphism: London, Journal of Geological Society, v. 155, p. 1025–1036.

Brueckner, H., and van Roermund, H., 2004, Dunk tectonics: A multiple subduction/eduction model for the evolution of the Scandinavian Caledonides: Tectonics, v. 23, doi: 10.1029/2003TC001502.

Brueckner, H., Medaris, G., and Bakun-Czubarow, N., 1991, Nd and Sr age and isotopic patterns from Variscan eclogites of the eastern Bohemian Massif: Neues Jahrb für Mineralogie, Abhandlungen, v. 163, p. 169–196.

Brueckner, H., Blusztajn, J., and Bakun-Czubarow, N., 1996, Trace-element and Sm-Nd age zoning in garnets from peridotites of Caledonia and Variscan mountains and tectonic implications: Journal of Metamorphic Geology, v. 14, p. 61–73.

Chemenda, A., Mattauer, M., and Bokun, A., 1996, Continental subduction and a mechanism for exhumation of high-pressure metamorphic rocks: New modelling and field data from Oman: Earth and Planetary Science Letters, v. 143, 173–182.

Crowley, Q. G., Timmermann, H., Noble, S. R., and Holland, J. G., 2002, Palaeozoic terrane amalgamation in Central Europe: a REE and Sm-Nd isotopic study of the pre-Variscan basement, NE Bohemian Massif, *in* Winchester, J. A., Pharaoh, T. C., and Verniers, J., editors, Palaeozoic Amalgamation of Central Europe: London, Geological Society Special Publication, v. 201, p. 157–176.

Cwojdzinski, S., 1982, Ewolucja strukturalna wschodniej czesci Ziemi Klodzkiej w swietle nowej interpretacji faldów najstarszych generacji: Biuletyn Institutu Geologii, v. 341, p. 169–182.

Cymerman, Z., 1987, Connection of the Sleza ophiolite with the Variscan structure of the Sowie metamorphic rocks: Przeglad Geologia, v. 6, p. 304–312.

——— 1997, Structure, kinematics, and an evolution of the Orlica-Snieznik Dome, Sudetes: Prace Panstwowego Instytutu Geologicznego CLVI, 107 p.

——— 1998, The Góry Sowie Terrane: a key to understanding the Palaeozoic evolution of the Sudetes area and beyond: Geological Quarterly, v. 42, p. 379–400.

Cymerman, Z., and Piasecki, M. A. J., 1994, The terrane concept in the Sudetes, Bohemian Massif: Geological Quarterly, v. 38, p. 191–210.

Cymerman, Z., Piasecki, M. A. J., and Seston, R., 1997, Terranes and terrane boundaries in the Sudetes, northeast Bohemian Massif: Geological Magazine, v. 134/5, p. 717–725.

Deino, A., Potts, R., 1990, Single-Crystal $^{40}Ar/^{39}Ar$ dating of the Olorgesailie Formation, Southern Kenya Rift: Journal of Geophysical Research, v. 95, p. 8453–8470.

Don, J., Dumicz, M., Wojciechowska, I., and Zelazniewicz, A., 1990, Lithology and tectonics of the Orlica-Snieznik dome, Sudetes – recent state of knowledge: Neues Jahrbuch für Geologie und Paläontologie, Abhandlungen, v. 179, p. 159–188.

Dubinska, E., Bylina, P., Kozlowski, A., Dörr, W., and Nejbert, K., 2004, U-Pb dating of serpentinization: hydrothermal zircon from a metasomatic rodingite shell (Sudetic ophiolite, SW Poland): Chemical Geology, v. 203, p. 183–203.

Franke, W., and Stein, E., 2000, Exhumation of high-grade rocks in the Saothuringian Belt: geological constraints and geodynamic concepts, *in* Franke, W., Haak., V., Oncken, O., and Tanner, D., editors, Orogenic processes: Quantification and modeling in the Variscan Belt: London, Geological Society Special Publications, v. 179, p. 337–354.

Franke, W., and Zelazniewicz, A., 2000, The eastern termination of the Variscides terrane correlation and kinematic evolution, *in* Franke, W., Haak., V., Oncken, O., and Tanner, D., editors, Orogenic processes: Quantification and modeling in the Variscan Belt: London, Geological Society Special Publication, v. 179, p. 63–86.

——— 2002, Structure and evolution of the Bohemian Arc, *in* Winchester, J. A., Pharaoh, T. C., and Verniers, J., editors, Palaeozoic Amalgamation of Central Europe: London, Geological Society Special Publication, v. 201, p. 279–293.

Glascock, J., ms, 2004, Exhumation of the Orlica-Sneznik Dome, northeastern Bohemian massif (Czech Republic and Poland): Athens, Ohio, Ohio University, Masters thesis, 80 p.

Gordon, S. M., Schneider, D. A., Manecki, M., and Holm, D. K., 2005, Exhumation and metamorphism of an ultrahigh-grade terrane: geochronometric investigations of the Sudete Mountains (Bohemia), Poland and Czech Republic: London, Journal of the Geological Society, v. 162, p. 841–855.

Gunia, T., 1990, Acritarcha and microprolematica of the crystalline limestones from the vicinity of Romanowo Gorne (central Sudete Mountains): Geologia Sudetica, v. 24, p. 101–137, (in Polish, with English summary).

Jamrozik, L., 1981, Tectonic position of ultrabasite-basite massifs surrounding the Góry Sowie Mts. Block, *in* Narebski, W., editor, Ophiolites and initialites of the northern border of the Bohemian massif: Guidebook for excursions, May-June 1981, v. 2, p. 86–95.

Józefiak, D., 2000, Geothermobarometry in staurolite-grade mica schists from the southern part of the Niemcza-Kamieniec Metamorphic Complex (Fore-Sudetic Block, SW Poland): Neues Jahrbuch für Mineralogie, Abhandlungen, v. 175, p. 223–248.

Kossmat, F., 1925, Erscheinungen und Probleme des Uberschiebungsbaues in varistischen Gebirgen Sachsens und der Sudetenländer: Zentralblatt für Mineralogie, B, p. 348–358.

——— 1927, Gliederung des varistischen Gebirgsbaues: Abhandlungen des sächsischen geologischen Landesantes, v. 1, p. 1–39.

Kozlowski, A., and Bakun-Czubarow, N., 1997, Fluidy w mineralach asocjacji eklogitowych z rejonu Sniewznika: Polskie Towarzystwo Mineralogiczne – Prace Specjalne, v. 9, p. 114–115.

Kröner, A., and Hegner, E., 1998, Geochemistry, single zircon ages and Sm-Nd systematics of granitoid rocks form the Góry Sowie (Owl Mts), Polish West Sudetes: evidence for early Palaeozoic arc-related plutonism: London, Journal of the Geological Society, v. 155, p. 711–724.

Kröner, A., Hegner, E., Hammer, J., Haase, G., Bielicki, K. H., Krauss, M., and Eidam, J., 1994a, Geochronology and Nd-Sr systematics of Lusatian granitoids: significance for the evolution of the Variscan orogen in east-central Europe: Geologische Rundschau, v. 83, p. 357–376.

Kröner, A., Jaeckel, P., and Opletal, M., 1994b, Pb-Pb and U-Pb zircon ages for orthogneisses from eastern Bohemia: further evidence for a major Cambro-Ordovician magmatic event: Journal of the Czech Geological Society, v. 39, p. 61.

Kröner, A., Jaeckel, P., Hegner, E., and Opletal, M., 2001, Single zircon ages and whole-rock Nd isotopic systematics of Early Paleozoic granioid gneisses from the Czech and Polish Sudetes (Jizerske hory, Krkonose and Orlice-Sneiznik Complex): International Journal of Earth Science, v. 90, p. 304–324.

Kryza, R., Pin, C., and Vielzeuf, D., 1996, High pressure granulites from the Sudetes (SW Poland): evidence of crustal subduction and collisional thickening in the Variscan Belt: Journal of Metamorphic Geology, v. 14, p. 531–546.

Lange, U., Bröcker, M., Mezger, K., and Don, J., 2002, Geochemistry and Rb-Sr geochronology of a ductile shear zone in the Orlica-Snieznik dome (West Sudetes, Poland): International Journal of Earth Sciences, v. 91, p. 1005–1016.

Maluski, H., and Patocka, F., 1997, Geochemistry and $^{40}Ar/^{39}Ar$ geochronology of the mafic metavolcanic rocks from the Rychory Mountains complex (West Sudetes, Bohemian Massif): paleotectonic significance: Geological Magazine, v. 134, p. 703–716.

Maluski, H., Rajlich, P., and Soucek, J., 1995, Pre-variscan, Variscan and Early Alpine thermo-tectonic history of the north-eastern Bohemian Massif: An $^{40}Ar/^{39}Ar$ study: Geologische Rundschau, v. 84, p. 345–358.

Marcoline J., Heizler M., Goodwin, L. B., Ralser S., and Clark J., 1999, Thermal, structural and petrological evidence for 1.4 Ga metamorphism and deformation in central New Mexico: Rocky Mountain Geology, v. 34, p. 93–119.

Marheine, D., Kachlík, V., Maluski, H., Patoçka, F., and Zelazniewicz, A., 2002, New $^{40}Ar/^{39}Ar$ ages in the West Sudetes (Bohemian Massif): constraints on the Variscan polyphase tectonothermal development, *in* Winchester, J. A., Pharaoh, T. C., and Verniers, J., editors, Palaeozoic Amalgamation of Central Europe: London, Geological Society Special Publications, v. 201, p. 133–156.

Matte, P., Maluski, H., Rajlich, P., and Franke, W., 1990, Terrane boundaries in the Bohemian Massif: result of large-scale Variscan shearing: Tectonophysics, v. 77, p. 151–170.

Mazur, S., and Puziewicz, J., 1995, Mylonites of the Niemcza Zone: Annales Societatis Geologorum poloniae, v. 64, p. 23–52, (in Polish, with English summary).

McDougall, I., and Harrison, T. M., 1999, Geochronology and Thermochronology by the $^{40}Ar/^{39}Ar$ Method, 2nd edition: New York, Oxford University Press, p. 1–43.

Oberc, J., 1991, Problem of non-rooted Variscan nappes of crystalline basement from Lower Silesia: Pzeglad Geologia, v. 10, p. 437–446.

O'Brien, P. J., Kröner, A., Jaeckel, P., Hegner, E., Zelazniewicz, A., and Kryza, R., 1997, Petrological and isotopic studies on Palaeozoic high-pressure granulies, Góry Sowie Mts, Polish Sudetes: Journal of Petrology, v. 38, p. 433–456.

Oliver, G. J. H., and Kelley, S., 1993, $^{40}Ar/^{39}Ar$ fusion ages from the Polish Sudetes: Variscan tectonothermal reworking of Caledonian protoliths: Neues Jahrbuch für Geologie und Paläontologie, Monatshefte, 1993, p. 321–334.

Oliver, G. J. H., Corfu, F., and Krogh, T. E., 1993, U-Pb ages from SW Poland: evidence for a Caledonian suture zone between Baltica and Gondwana: London, Journal of the Geological Society, v. 150, p. 355–369.

Patocka, F., Pivec, E., and Oliveriova, D., 1996, Mineralogy and petrology of mafic blueschists from the Rychory Mts crystalline complex (Western Sudetes, Bohemian Massif): Neues Jahrbuch für Mineralogie, Abhandlungen, v. 170, p. 313–320.

Porebski, S. J., 1981, Swiebodzice succession (Upper Devonian-Lowest Carboniferous): a prograding, mass flow dominated fan-delta complex: Geologia Sudetica, v. 16, p. 101–192, (in Polish, with English summary).

——— 1990, Onset of coarse clastic sedimentaion in the Variscan realm of the Sudetes (SW Poland): an example from the Upper Devonian-Lower Carboniferious Swiebodzice succession: Neues Jahrbuch für Geologie und Paläontologie, Abhandlungen, v. 179, p. 259–274.

Pressler, R. E., Petronis, M., Schneider, D. A., and Holm, D. K., 2005a, An integrated petrofabric study of the high-pressure Orlica-Snieznik complex, Czech Republic and Poland: Geological Society of America, Abstracts, v. 37, p. 211.

Pressler, R. E., Petronis, M. S., Schneider, D. A., Holm, D. K., and Manecki, M., 2005b, An exhumed mid-crustal attachment zone: Results of AMS fabric analysis of the Orlica-Snieznik massif, Poland and Czech Republic: Geophysical Research Abstracts, v. 7, p. 72.

Schulmann, K., and Gayer, R., 2000, A model for a continental accretionary wedge developed by oblique collision: the NE Bohemian Massif: London, Journal of the Geological Society, v. 157, p. 401–416.

Smulikowski, K., and Bakun-Czubarow, N., 1969, Corundum-bearing eclogite amphibolite forming a loaf-shaped inclusion in the granulites of Bystrzyca Górna (Góry Sowie, Middle Sudetes, Poland): Bulletin de l'Académie Polonaise des Sciences, Série des Sciences Géologiques et Geographiques, v. 17, p. 1–6.

Steiger R., and Jaeger, E., 1977, Subcommission on Geochronology: Convention on the use of decay constants in geo and cosmochronology: Earth and Planetary Science Letters, v. 36, p. 359–362.

Steltenpohl, M. G., Cymerman, Z., Krogh, E., and Kunk, M. J., 1993, Exhumation of eclogitized continental basement during Variscan lithospheric delamination and gravitational collapse, Sudety Mountains, Poland: Geology, v. 21, p. 1111–1114.

Stípská, P., Schulmann, K., and Kröner, A., 2004, Vertical extrusion and middle crustal spreading of omphacite granulite: a model of syn-convergent exhumation (Bohemian Massif, Czech Republic): Journal of Metamorphic Geology, v. 22, p. 179–198.

Svoboda, J., and Chaloupsky, J., 1966, The West Sudeten Crystalline, *in* Svoboda, J., Dvorak, J., Havlena, V., Havlicek, V., Horny, R., Chlupac, I., Klein, V., Kopecky, L., Malecha, A., Malkovsky, M., Soukup, J., Tásler, R., Václ, J., and Zebera, K., editors, Regional geology of Czechoslovakia I: Prague, Geological Survey, p. 215–278.

Szczepanski, J., Anczkiewicz, R., Mazur, S., and Thirlwall, M., 2004, Timing of ultrahigh-pressure metamorphism in the Orlica-Snieznik Dome, West Sudetes: Special Papers, Mineralogical Society of Poland, v. 24, p. 365–368.

Teisseyre, J. H., 1973, Metamorphic complex of Rudawy Janowickie and Lasocki Grzbiet ridge: Geologia Sudetica, v. 8, p. 7–129.

Timmerman, H., Parrish, R., Noble, S., and Kryza, R., 2000, New U-Pb monazite and zircon data from the Sudete Mountains in SW Poland: evidence for a single-cycle Variscan orogeny: London, Journal of the Geological Society, v. 157, p. 265–268.

Turniak, K., Mazur, S., and Wysoczanski, R., 2000, SHRIMP zircon geochronology and geochemistry of the Orlica-Snieznik gneisses (Variscan belt of Central Europe) and their tectonic implications: Geodinamica Acta, v. 13, p. 293–312.

van Breemen, O., Bowes, D. R., Aftalion, M., and Zelazniewicz, A., 1988, Devonian tectonothermal activity in the Góry Sowie gneissic block, Sudetes, southwestern Poland: evidence from Rb-Sr and U-Pb isotopic studies: Annales Societatis Geologorum Poloniae, v. 58, p. 3–19.

Vannay, J. C., and Grasemann, B., 2001, Himalayan inverted metamorphism and syn-convergence extension as a consequence of a general shear extrusion: Geological Magazine, v. 138, p. 253–276.

Walsh, E., and Hacker, B., 2004, The fate of subducted continental margins: Two-stage exhumation of the high-pressure to ultrahigh-pressure Western Gneiss Region, Norway: Journal of Metamorphic Geology, v. 22, p. 671–687.

Zahniser, S., ms, 2004, Tectonometamorphic evolution of an allochthonous terrane, Sowie Góry, northeastern Bohemian massif (Poland): Athens, Ohio University, Masters thesis, 76 p.

Zakowa, H., 1963, Stratigraphy and facial extent of the Lower Carboniferous in the Sudetes Mountains: Kwartalnik Geologii, v. 7, p. 73–94.

Zelazniewicz, A., 1985, Granulitic inliers amidst a gneissic-migmatitic complex of the Owl Mts., Sudetes: Acta Geologica Polonica, v. 35, p. 157–171.

——— 1987, Tectonic and metamorphic evolution of the Góry Sowie, Sudetes Mts., SW Poland: Annales Societatis Geologorum Poloniae, v. 57, p. 203–348.

——— 1990, Deformation and metamorphism in the Góry Sowie gneiss complex, Sudetes, SW Poland: Neues Fahrbuch für Geologie und Paläontologie, Abhandlungen, v. 179, p. 129–157.

——— 1997, The Sudetes as a Paleozoic orogen in central Europe: Geological Magazine, v. 134, p. 691–702.

Zelazniewicz, A., Dorr, W., and Dubinska, E., 1998, Lower Devonian oceanic crust from U-Pb zircon evidence and Eo-Variscan event in the Sudetes, *in* Franke, W., and Herzberg, S., editors, SPP Orogene Processe 7. Kolloquium, Giessen: Terra Nostra, v. 98/2, p. 173–176.

Znosko, J., 1981, The problem of oceanic crust and of ophiolites in the Sudetes: Bulletin de l'Academie Polonaise des Sciences, serie Sciences de la Terre, v. 29, p. 185–197.

APPENDIX 1

$^{40}Ar/^{39}Ar$ analytical isotopic and age data for the Góry (gs-), Orlica (O-), and Snieznik (sz-) massifs

ID	Power (Watts)	$^{40}Ar/^{39}Ar$	$^{37}Ar/^{39}Ar$	$^{36}Ar/^{39}Ar$ (x 10^{-3})	$^{39}Ar_K$ (x 10^{-15} mol)	K/Ca	$^{40}Ar^*$ (%)	^{39}Ar (%)	Age (Ma)	±1s (Ma)
$^{40}Ar/^{39}Ar$ analytical isotopic data for the Gory Sowie Block										
GS-2C biotite, 0.82 mg, J=0.0161537										
A	650	6.30	0.0102	5.265	5.1	50	75.2	1.1	132.5	1.6
B	750	13.66	0.0025	0.901	30.5	202	98.0	7.8	352.7	1.0
C	850	14.51	0.0009	0.128	69.6	580	99.7	22.9	378.3	1.2
D	920	14.52	0.0009	0.118	47.8	568	99.8	33.4	378.8	0.8
E	1000	14.76	0.0014	0.177	34.9	376	99.6	41.0	383.9	0.6
F	1075	14.94	0.0013	0.131	53.2	398	99.7	52.5	388.5	0.9
G	1110	14.76	0.0009	0.157	65.1	553	99.7	66.7	384.2	1.0
H	1180	14.62	0.0007	0.154	79.4	723	99.7	84.0	380.8	0.6
I	1210	14.57	0.0006	0.052	42.9	876	99.9	93.4	380.4	0.6
J	1250	14.64	0.0004	-0.057	27.2	1375	100.1	99.3	382.8	1.2
K	1300	14.81	-0.0016	0.044	3.3	-	99.9	100.0	386.0	2.3
Integrated age ± 1s			n=11		458.8		K2O=13.31 %		377.5	0.5
Plateau ± 1s		steps C-K	n=9	MSWD=12.59					**382.1**	**1.0**
GS-6 biotite, 0.49 mg, J=0.0161099										
A	650	4.22	0.2818	7.071	18.6	1.8	50.8	4.6	60.9	1.1
B	750	13.13	0.0590	2.946	30.3	8.6	93.4	12.0	324.8	0.8
C	850	14.59	0.0368	1.154	34.7	13.9	97.7	20.6	372.3	0.8
D	920	15.18	0.0309	0.827	33.1	16.5	98.4	28.8	388.3	0.6
E	1000	15.69	0.0656	0.980	32.7	7.8	98.2	36.8	399.4	0.7
F	1075	16.20	0.1137	0.639	71.0	4.5	98.9	54.3	413.6	0.5
G	1110	15.66	0.1072	0.519	36.2	4.8	99.1	63.2	401.9	0.9
H	1180	14.87	0.0707	0.371	99.3	7.2	99.3	87.7	384.4	0.7
I	1210	14.73	0.0859	0.148	38.5	5.9	99.7	97.2	382.7	0.6
J	1250	14.41	0.1334	0.910	8.1	3.8	98.2	99.2	369.9	1.3
K	1300	15.84	0.1221	3.063	3.2	4.2	94.3	100.0	388.5	2.5
Integrated age ± 1s			n=11		405.8		K2O=19.74 %		**373.2**	**0.5**
Plateau ± 1s				MSWD=N/A					N/A	N/A
GS-6 hornblende, 5.34 mg, J=0.0160577										
A	800	44.11	2.6391	38.752	1.9	0.19	74.5	0.8	765.2	6.7
B	900	35.29	3.1815	31.042	1.0	0.16	74.7	1.2	637.8	8.2
C	1000	19.79	5.8213	7.257	1.8	0.09	91.5	1.9	461.7	4.7
D	1030	17.04	5.2772	6.330	1.6	0.10	91.5	2.6	403.8	4.5
E	1060	15.79	5.4233	2.489	13.4	0.09	98.1	8.0	401.4	1.2
F	1090	15.46	4.9477	1.691	67.2	0.10	99.3	35.1	398.2	0.7
G	1120	14.82	4.6575	1.399	82.0	0.11	99.7	68.2	384.6	1.1
H	1170	15.45	5.5418	2.447	15.7	0.09	98.2	74.6	394.0	1.3
I	1200	15.19	5.2261	1.855	52.8	0.10	99.1	96.0	391.3	0.8
J	1250	14.18	5.4627	-1.539	0.6	0.09	106.3	96.2	391.7	9.8
JJ	1250	14.96	5.2953	1.671	9.4	0.10	99.5	100.0	387.5	1.8
Integrated age ± 1s			n=11		247.5		K2O=1.11 %		396.4	0.7
Plateau ± 1s		steps G-JJ	n=5	MSWD=9.23					**389.9**	**1.7**
GS-10 biotite, 1.19 mg, J=0.0160556										
A	650	11.50	0.0120	4.746	6.5	42	87.8	1.1	270.4	1.7
B	750	14.97	0.0023	0.960	36.1	221	98.1	7.4	381.4	0.8
C	850	14.51	0.0007	0.183	132.7	756	99.6	30.4	375.8	0.5
D	920	14.56	0.0005	0.162	69.4	1077	99.7	42.5	377.3	1.0
E	1000	14.80	0.0011	0.401	40.8	465	99.2	49.5	381.2	0.7
F	1075	14.80	0.0011	0.350	76.9	459	99.3	62.9	381.6	0.7
G	1110	14.69	0.0005	0.195	60.0	1064	99.6	73.3	380.2	0.9
H	1180	14.58	0.0004	0.259	93.2	1390	99.5	89.5	377.1	0.6
I	1210	14.62	0.0004	0.200	42.2	1323	99.6	96.8	378.4	0.5
J	1250	14.72	0.0015	0.233	16.5	334	99.5	99.6	380.6	0.9
K	1300	15.13	0.0145	1.193	2.0	35	97.7	100.0	383.4	3.1
Integrated age ± 1s			n=11		576.3		K2O=11.59 %		377.4	0.5
Plateau ± 1s		steps B-K	n=10	MSWD=10.58					**378.9**	**0.7**

APPENDIX 1
(continued)

ID	Power (Watts)	$^{40}Ar/^{39}Ar$	$^{37}Ar/^{39}Ar$	$^{36}Ar/^{39}Ar$ (x 10^{-3})	$^{39}Ar_K$ (x 10^{-15} mol)	K/Ca	$^{40}Ar^*$ (%)	^{39}Ar (%)	Age (Ma)	±1s (Ma)
GS-12 biotite, 1.79 mg, J=0.0160803										
A	650	7.69	0.0119	5.653	15.0	43	78.2	1.9	166.0	1.0
B	750	14.74	0.0097	1.496	57.6	53	97.0	8.9	372.8	1.4
C	850	14.46	0.0011	0.434	171.9	478	99.1	30.1	373.6	1.2
D	920	14.50	0.0011	0.260	82.7	480	99.5	40.3	375.6	0.7
E	1000	14.65	0.0015	0.465	65.1	345	99.1	48.3	377.8	0.7
F	1075	14.66	0.0014	0.298	165.3	354	99.4	68.6	379.1	0.7
G	1110	14.63	0.0011	0.301	81.5	449	99.4	78.7	378.5	0.8
H	1180	14.59	0.0009	0.302	122.4	538	99.4	93.7	377.6	1.0
I	1210	14.57	0.0013	0.175	43.8	384	99.6	99.1	378.0	0.7
J	1250	14.79	0.0148	0.289	7.2	34	99.4	100.0	382.5	1.4
Integrated age ± 1s			n=10		812.6		K2O=10.84 %		373.0	0.6
Plateau ± 1s		steps E-I	n=5	MSWD=0.65					**378.3**	**0.7**
GS-12 muscovite, 0.48 g, J=0.0160824										
C	700	16.05	0.0027	3.780	4.4	189	93.0	0.5	387.7	2.1
D	750	15.93	0.0021	3.201	10.1	240	94.1	1.6	388.8	1.5
E	800	15.62	0.0014	3.016	18.7	359	94.3	3.6	382.9	1.1
F	840	15.04	0.0007	1.766	29.3	727	96.5	6.7	377.9	1.3
G	880	14.94	0.0004	1.888	56.6	1238	96.3	12.9	374.9	1.0
H	920	14.39	0.0002	0.504	182.5	2878	99.0	32.6	371.4	0.6
I	960	14.56	0.0003	0.515	55.0	1994	99.0	38.5	375.3	0.6
J	1000	14.68	0.0003	0.691	41.2	1696	98.6	43.0	376.9	0.6
K	1040	14.53	0.0000	0.435	38.3	-	99.1	47.1	375.3	1.1
L	1080	14.51	0.0002	0.525	52.7	2827	98.9	52.8	374.1	0.9
M	1120	14.43	0.0001	0.536	74.2	3492	98.9	60.8	372.1	0.8
N	1160	14.54	0.0002	0.595	77.2	2886	98.8	69.1	374.3	0.7
O	1200	14.43	0.0002	0.204	80.2	2642	99.6	77.8	374.6	0.7
P	1250	14.45	0.0001	0.163	80.2	5047	99.7	86.5	375.3	1.0
Q	1350	14.28	0.0002	0.163	72.7	2894	99.7	94.3	371.2	1.2
R	1650	15.26	0.0001	3.228	52.7	6192	93.7	100.0	372.9	1.3
Integrated age ± 1s			n=16		925.9		K2O=32.22 %		374.1	0.5
Plateau ± 1s		steps H-R	n=11	MSWD=5.94					**374.1**	**0.7**
GS-16A hornblende, 5.78 mg, J=0.016084										
A	800	80.57	28.1421	207.364	0.4	0.02	26.7	0.5	545.4	32.2
B	900	18.96	30.6652	23.063	0.3	0.02	76.9	0.9	387.2	16.6
C	1000	13.69	10.5463	11.378	1.4	0.05	81.6	2.7	299.5	7.4
D	1030	13.62	12.6098	5.266	0.6	0.04	96.0	3.5	346.4	9.6
E	1060	15.69	16.9031	8.617	2.4	0.03	92.4	6.6	381.4	3.8
F	1090	14.72	17.6780	5.682	38.4	0.03	98.2	56.4	380.6	1.5
G	1120	14.83	18.2878	6.729	9.0	0.03	96.4	68.1	377.2	2.5
H	1170	15.72	18.4690	13.790	1.6	0.03	83.4	70.2	348.9	6.6
I	1200	14.88	17.8542	5.779	12.4	0.03	98.1	86.2	384.2	1.7
J	1250	14.97	18.2245	6.550	10.6	0.03	96.8	100.0	381.8	2.1
Integrated age ± 1s			n=10		77.1		K2O=0.32 %		379.5	1.5
Plateau ± 1s		steps E-G	n=3	MSWD=0.78					**379.9**	**1.3**
GS-16B biotite, 1.85 mg, J=0.01615										
A	650	8.93	0.0934	9.631	6.9	5	68.1	0.8	168.7	1.8
B	750	14.47	0.0067	1.325	78.2	76	97.3	9.9	369.1	0.6
C	850	14.23	0.0015	0.180	118.9	337	99.6	23.7	371.2	0.6
D	920	14.26	0.0016	0.121	143.4	322	99.7	40.4	372.4	0.6
E	1000	14.38	0.0034	0.150	57.0	148	99.7	47.0	375.1	0.8
F	1075	14.44	0.0069	0.137	114.6	74	99.7	60.3	376.6	0.6
G	1110	14.24	0.0050	0.081	113.7	102	99.8	73.5	372.3	0.8
H	1180	14.28	0.0085	0.161	94.8	60	99.7	84.5	372.6	0.6
I	1210	14.19	0.0030	0.082	85.9	169	99.8	94.5	371.1	0.6
J	1250	14.32	0.0029	0.138	41.1	175	99.7	99.3	373.7	0.7
K	1300	14.50	0.0020	0.174	6.1	262	99.6	100.0	377.8	1.6
Integrated age ± 1s			n=11		860.6		K2O=11.06 %		371.1	0.5
Plateau ± 1s		steps C-K	n=9	MSWD=8.59					**373.0**	**0.8**

APPENDIX 1
(continued)

ID	Power (Watts)	$^{40}Ar/^{39}Ar$	$^{37}Ar/^{39}Ar$	$^{36}Ar/^{39}Ar$ (x 10^{-3})	$^{39}Ar_K$ (x 10^{-15} mol)	K/Ca	$^{40}Ar^*$ (%)	^{39}Ar (%)	Age (Ma)	±1s (Ma)
GS-16B muscovite, 0.14g, J=0.0163863										
A	600	33.64	0.6348	107.333	0.7	1	5.8	0.5	56.8	23.2
B	650	15.90	0.3564	23.483	0.4	1	56.5	0.8	247.3	15.1
C	700	15.62	0.2007	7.126	0.4	3	86.6	1.0	360.7	14.1
D	750	15.98	0.0665	0.181	1.3	8	99.7	1.9	417.8	5.5
E	800	15.03	0.0108	1.465	2.0	47	97.1	3.2	386.3	3.9
F	840	14.59	0.0088	1.548	2.7	58	96.9	4.9	375.3	2.8
G	880	14.27	0.0021	0.582	5.8	239	98.8	8.7	374.2	1.9
H	920	14.21	0.0009	0.361	28.1	555	99.2	27.0	374.6	0.9
I	960	13.89	0.0016	0.368	24.1	325	99.2	42.8	366.7	1.1
J	1000	13.83	0,0023	0.402	14.5	223	99.1	52.3	364.9	1.2
K	1040	14.06	0.0040	0.720	6.8	127	98.5	56.7	368.2	1.5
L	1080	14.29	0.0058	0.975	7.1	88	98.0	61.4	372.0	1.4
M	1120	14.28	0.0049	0.732	6.8	104	98.5	65.8	373.6	1.2
N	1160	14.47	0.0034	1.349	10.9	152	97.2	72.9	373.8	1.0
O	1200	14.38	0.0028	0.597	16.1	182	98.8	83.4	376.9	0.9
P	1250	14.48	0.0024	0.610	10.1	210	98.8	90.0	379.2	1.3
Q	1350	14.90	0.0006	2.425	5.4	829	95.2	93.5	376.3	1.9
R	1650	16.17	0.0001	7.129	9.9	4845	86.9	100.0	373.4	1.7
Integrated age ± 1s			n=18		153.1		K2O=8.38 %		371.2	0.6
Plateau ± 1s		steps L-R	n=7	MSWD=2.7					**375.0**	**1.5**
GS-18 biotite, 0.66 mg, J=0.0161784										
A	650	10.91	0.0275	20.751	1.9	19	43.7	0.5	133.7	6.8
B	750	11.98	0.0118	4.952	10.0	43	87.8	3.1	282.9	1.4
C	850	12.84	0.0047	1.028	37.7	108	97.6	12.8	332.6	0.7
D	920	12.92	0.0046	0.435	51.7	112	99.0	26.0	338.6	0.6
E	1000	12.93	0.0080	0.795	33.6	63	98.2	34.7	336.3	0.6
F	1075	12.96	0.0125	0.866	42.4	41	98.0	45.6	336.7	0.7
G	1110	12.85	0.0228	0.899	28.7	22	97.9	53.0	333.8	0.7
H	1180	12.86	0.0189	1.026	50.7	27	97.7	66.0	333.2	0.6
I	1210	12.89	0.0169	0.556	42.3	30	98.7	76.9	337.2	0.7
J	1250	12.87	0.0479	0.192	64.9	11	99.6	93.6	339.3	0.6
K	1300	12.90	0.1047	0.341	17.6	5	99.3	98.1	339.1	0.9
L	1650	14.52	0.0345	5.474	7.5	15	88.9	100.0	341.6	1.5
Integrated age ± 1s			n=12		389.0		K2O=13.99 %		334.3	0.5
Plateau ± 1s		steps D-L	n=9	MSWD=12.73					**336.8**	**0.9**
GS-18 hornblende, 5.73 mg, J=0.0161763										
A	800	13.53	0.3444	5.546	11.5	1.48	88.1	3.2	317.4	1.6
B	900	12.08	0.5088	1.812	13.3	1.00	95.9	6.9	309.5	1.3
C	1000	11.82	1.8135	1.977	11.0	0.28	96.3	10.1	304.6	1.5
D	1030	12.42	2.1164	2.784	7.1	0.24	94.7	12.2	314.1	2.3
E	1060	12.61	3.0973	1.986	10.1	0.16	97.3	15.2	326.7	1.6
F	1090	12.81	4.6594	1.902	44.9	0.11	98.5	29.3	335.4	0.7
G	1120	12.76	4.4159	1.567	97.6	0.12	99.1	64.5	336.3	1.3
H	1170	12.83	3.6705	1.714	19.9	0.14	98.3	72.5	335.2	1.1
I	1200	12.86	4.0726	1.709	13.2	0.13	98.6	78.0	337.0	1.3
J	1250	12.92	4.9075	1.869	48.1	0.10	98.8	99.6	338.9	0.7
K	1300	15.50	4.9327	10.442	0.9	0.10	82.6	100.0	340.1	16.4
Integrated age ± 1s			n=11		277.6		K2O=1.15 %		332.4	0.7
Plateau ± 1s		steps F-K	n=6	MSWD=2.87					**336.8**	**0.8**
GS-21 biotite, 0.98 mg, J=0.0161079										
A	650	5.20	0.0094	5.112	14.8	54	70.8	4.4	103.6	1.1
B	750	9.96	0.0030	2.610	38.2	169	92.2	15.7	248.4	1.0
C	850	10.53	0.0019	0.989	61.8	272	97.2	33.9	274.8	0.5
D	920	10.84	0.0024	1.147	28.6	213	96.9	42.3	281.2	0.7
E	1000	10.66	0.0033	1.556	36.0	156	95.7	52.9	273.7	0.6
F	1075	10.66	0.0021	1.609	69.6	245	95.5	73.5	273.5	0.8
G	1110	10.42	0.0018	1.569	29.5	282	95.5	82.2	267.6	0.7
H	1180	10.57	0.0017	1.331	50.2	308	96.3	97.0	273.3	0.8
I	1210	11.18	0.0031	0.717	10.2	167	98.1	100.0	293.0	0.9
Integrated age ± 1s			n=9		338.9		K2O=8.25 %		264.6	0.4
Plateau ± 1s		steps C-H	n=6	MSWD=39.52					**274.3**	**1.7**

APPENDIX 1
(continued)

ID	Power (Watts)	$^{40}Ar/^{39}Ar$	$^{37}Ar/^{39}Ar$	$^{36}Ar/^{39}Ar$ (x 10^{-3})	$^{39}Ar_K$ (x 10^{-15} mol)	K/Ca	$^{40}Ar^*$ (%)	^{39}Ar (%)	Age (Ma)	±1s (Ma)
$^{40}Ar/^{39}Ar$ analytical isotopic data for the Orlica Sneiznik Complex										
SZX-6 biotite, 0.47 mg, J=0.0162489										
A	650	10.74	0.0393	8.123	15.0	13	77.6	3.5	228.7	1.4
B	750	12.37	0.0027	1.151	50.6	188	97.2	15.4	321.6	0.6
C	850	12.54	0.0009	0.445	61.5	595	98.9	29.8	330.6	0.6
D	920	12.70	0.0010	0.334	37.8	488	99.2	38.7	335.3	0.7
E	1000	12.65	0.0012	0.400	55.7	437	99.1	51.8	333.7	0.9
F	1075	12.60	0.0005	0.292	137.4	960	99.3	84.0	333.3	0.5
G	1110	12.71	0.0007	0.247	42.4	712	99.4	94.0	336.4	0.6
H	1180	12.82	0.0020	1.175	16.4	257	97.3	97.8	332.4	1.0
I	1210	12.63	0.0064	1.147	5.0	80	97.3	99.0	327.9	1.5
J	1250	12.87	0.0617	1.716	2.7	8	96.1	99.6	329.9	2.7
K	1300	13.31	-0.0004	3.251	1.6	-	92.8	100	329.2	4.1
Integrated age ± 1s			n=11		426.1		K2O=21.43 %		328.4	0.5
Plateau ± 1s		steps D-I	n=6	MSWD=6.49					**334.2**	**0.8**
SZX-9 hornblende, 2.16 mg, J=0.0161262										
A	800	119.5	16.67	165.8	0.6	0.031	60.1	1.3	1399.1	14.3
B	900	25.39	14.56	44.1	0.3	0.035	53.2	2.0	358.7	21.7
C	1000	16.27	25.78	13.3	1.4	0.020	88.4	4.9	382.1	6.9
D	1030	16.26	39.92	14.9	1.0	0.013	92.5	6.9	401.3	11.4
E	1060	15.26	27.91	14.6	0.8	0.018	86.3	8.5	353.4	9.8
F	1090	15.68	28.82	10.7	8.5	0.018	94.6	26	393.4	2.8
G	1120	14.63	31.41	10.1	12.8	0.016	96.7	53	377.4	2.8
H	1170	13.86	29.56	21.5	0.5	0.017	71.2	54	271.2	16.5
I	1200	19.34	30.21	35.7	0.5	0.017	57.8	55	304.6	21.9
J	1250	16.00	31.33	11.5	19.7	0.016	94.5	96	400.9	2.6
K	1300	22.05	31.09	27.3	1.0	0.016	74.7	98	432.8	10.4
L	1650	116.6	19.23	360.7	0.8	0.027	9.90	100	311.7	28.4
Integrated age ± 1s			n=12		47.9		K2O=0.53 %		406.2	2.5
Plateau ± 1s		steps A-L	n=12	MSWD=N/A					N/A	N/A
SZX-10A biotite, 0.44 mg, J=0.01633										
A	650	9.28	0.1469	12.02	5.2	3	61.7	1.5	160.9	2.2
B	750	13.13	0.0118	1.57	20.6	43	96.5	7.3	338.7	0.8
C	850	12.57	0.0037	0.38	71.3	137	99.1	27.7	333.5	0.5
D	920	12.81	0.0175	0.39	22.1	29	99.1	34.0	339.2	0.7
E	1000	12.75	0.0121	0.38	46.6	42	99.1	47.3	337.8	0.7
F	1075	12.64	0.0052	0.16	87.0	99	99.6	72.1	336.7	0.6
G	1110	12.79	0.0098	0.42	29.1	52	99.0	80.4	338.7	0.9
H	1180	12.74	0.0374	0.36	49.6	14	99.2	94.5	337.8	0.5
I	1210	12.80	0.0201	0.21	19.1	25	99.5	100.0	340.5	0.8
Integrated age ± 1s			n=9		350.5		K2O=18.74 %		334.5	0.5
Plateau ± 1s		steps D-I	n=6	MSWD=3.78					**338.2**	**0.5**
SZX-15 muscovite, 0.54 mg, J=0.0162816										
A	600	13.45	0.0739	18.76	2.1	7	58.8	0.8	218.1	13.5
B	650	14.63	0.0286	7.41	2.1	18	85.0	1.6	332.2	12.6
C	700	14.14	0.0070	5.19	2.4	73	89.1	2.5	336.3	11.1
D	750	13.78	0.0089	3.21	5.1	57	93.1	4.5	341.6	5.6
E	800	13.66	0.0026	2.35	8.8	199	94.9	7.9	345.1	3.3
F	840	13.30	0.0017	1.13	17.1	306	97.5	14.5	344.9	2.3
G	880	13.06	0.0010	0.79	16.5	493	98.2	20.8	341.4	1.9
H	920	12.92	0.0005	0.53	43.9	960	98.8	37.7	340.1	1.0
I	960	12.94	0.0005	0.58	60.0	1089	98.7	60.8	340.3	0.7
J	1000	12.90	0.0003	0.50	45.6	1836	98.9	78.4	339.7	1.5
K	1040	13.16	0.0007	1.21	15.0	779	97.3	84.2	340.9	1.8
L	1080	13.32	0.0012	1.15	13.2	419	97.4	89.3	345.3	2.2
M	1120	13.59	0.0024	1.76	6.8	209	96.2	91.9	347.5	4.1
N	1160	14.58	0.0077	3.02	3.9	66	93.9	93.4	362.3	6.9
O	1200	14.65	0.0078	1.32	2.4	66	97.3	94.4	376.0	10.0
P	1250	19.73	0.0185	2.27	2.1	28	96.6	95.2	487.0	11.4
Q	1350	21.85	0.0168	2.02	5.8	30	97.3	97.4	535.7	4.4
R	1650	19.86	0.0144	19.87	6.7	36	70.4	100.0	369.5	4.4
Integrated age ± 1s			n=18		259.7		K2O=11.34 %		347.6	0.7
Plateau ± 1s		steps B-M	n=12	MSWD=1.28					**340.9**	**0.5**

APPENDIX 1
(continued)

ID	Power (Watts)	$^{40}Ar/^{39}Ar$	$^{37}Ar/^{39}Ar$	$^{36}Ar/^{39}Ar$ (x 10^{-3})	$^{39}Ar_K$ (x 10^{-15} mol)	K/Ca	$^{40}Ar^*$ (%)	^{39}Ar (%)	Age (Ma)	±1s (Ma)
SZX-16 biotite, 1.26 mg, J=0.0162401										
A	650	11.17	0.0146	2.589	14.8	35	93.1	2.4	281.0	1.0
B	750	12.63	0.0022	0.316	65.4	230	99.3	12.9	333.6	0.5
C	850	12.45	0.0011	0.114	114.7	474	99.7	31.4	330.6	0.6
D	920	12.62	0.0022	0.202	60.7	228	99.5	41.2	334.2	0.7
E	1000	12.67	0.0039	0.150	58.2	130	99.7	50.5	335.8	0.8
F	1075	12.57	0.0028	0.136	122.3	184	99.7	70.2	333.6	0.6
G	1110	12.57	0.0035	0.163	65.8	144	99.6	80.8	333.4	0.6
H	1180	12.65	0.0107	0.206	53.1	48	99.5	89.4	335.0	0.6
I	1210	12.58	0.0205	0.092	37.3	25	99.8	95.4	334.1	0.6
J	1250	12.69	0.1634	0.310	19.2	3	99.4	98.4	335.6	0.8
K	1300	12.80	0.5062	0.634	9.7	1	98.9	100.0	336.6	1.4
Integrated age ± 1s			n=11		621.1		K2O=11.66 %		332.3	0.4
Plateau ± 1s		steps B-K	n=10	MSWD=5.45					**333.9**	**0.5**
SZX-18 biotite, 0.56 mg, J=0.0161578										
A	650	7.44	0.1504	6.186	9.9	3	75.5	1.3	156.3	1.7
B	750	13.06	0.0099	0.746	45.2	51	98.3	7.1	339.5	0.6
C	850	12.74	0.0036	0.160	132.3	142	99.6	24.0	336.0	0.6
D	920	12.77	0.0065	0.077	99.3	78	99.8	36.8	337.4	0.6
E	1000	12.85	0.0189	0.162	62.0	27	99.6	44.7	338.6	0.7
F	1075	12.95	0.0131	0.130	115.4	39	99.7	59.5	341.2	0.6
G	1110	12.80	0.0091	0.132	107.2	56	99.7	73.2	337.6	0.6
H	1180	12.76	0.0406	0.251	101.9	13	99.4	86.3	335.8	0.5
I	1210	12.70	0.0931	0.149	61.9	5	99.7	94.2	335.4	0.4
J	1250	12.81	0.2947	0.272	27.9	2	99.6	97.8	337.4	0.8
K	1300	12.98	0.1973	0.511	17.0	3	99.0	100.0	339.6	0.7
Integrated age ± 1s			n=11		780.0		K2O=33.11 %		335.5	0.4
Plateau ± 1s		steps B-K	n=10	MSWD=11.93					**337.6**	**0.6**
SZX-22B biotite, 0.34 mg, J=0.0163397										
A	650	12.46	0.0929	9.042	7.0	5	78.6	1.4	267.3	2.1
B	750	12.89	0.0019	0.510	65.8	263	98.8	14.2	340.5	0.5
C	850	12.68	0.0007	0.172	81.0	758	99.6	29.9	337.9	0.7
D	920	12.85	0.0009	0.247	33.0	596	99.4	36.3	341.5	1.3
E	1000	12.77	0.0009	0.209	63.4	598	99.5	48.6	339.8	0.7
F	1075	12.73	0.0004	0.097	131.1	1377	99.8	74.1	339.6	0.6
G	1110	12.65	0.0004	0.249	63.4	1221	99.4	86.4	336.6	1.3
H	1180	12.72	0.0008	0.357	60.7	656	99.2	98.2	337.5	0.8
I	1210	12.84	0.0109	0.602	9.1	47	98.6	100.0	338.6	1.2
Integrated age ± 1s			n=9		514.5		K2O=35.57 %		338.0	0.5
Plateau ± 1s		steps B-I	n=8	MSWD=2.61					**339.1**	**0.6**
SZX-22B muscovite, 0.38 mg, J=0.0162113										
A	600	10.13	0.2767	24.26	0.8	2	29.2	0.7	84.4	44.4
B	650	30.59	0.1530	57.37	0.4	3	44.6	1.0	359.9	75.4
C	700	16.01	0.0552	9.74	0.4	9	82.0	1.4	347.7	57.9
D	750	16.44	0.0128	11.25	1.3	40	79.7	2.4	347.1	20.7
E	800	14.48	0.0048	5.80	2.1	106	88.1	4.1	338.8	13.1
F	840	13.75	0.0026	4.56	4.2	193	90.2	7.6	329.9	6.4
G	880	13.00	0.0006	1.02	22.7	807	97.7	26.2	337.2	1.6
H	920	12.61	0.0010	0.54	32.5	517	98.7	52.9	331.1	1.7
I	960	13.54	0.0025	3.04	9.5	201	93.4	60.6	335.6	3.1
J	1000	13.28	0.0015	2.36	4.6	336	94.7	64.4	334.3	5.8
K	1040	13.02	0.0011	0.01	3.6	476	100.0	67.4	344.8	7.3
L	1080	13.31	0.0003	2.53	4.7	1831	94.4	71.3	333.8	5.7
M	1120	13.07	0.0003	1.15	7.1	1535	97.4	77.1	337.9	3.8
N	1160	13.32	0.0008	2.87	8.0	604	93.6	83.7	331.5	3.5
O	1200	13.05	0.0003	1.22	5.9	1952	97.2	88.5	336.9	4.5
P	1250	13.40	0.0015	2.80	4.5	331	93.8	92.2	334.2	5.9
Q	1350	13.27	0.0008	1.86	7.5	659	95.8	98.4	337.6	3.6
R	1650	30.97	0.0018	61.83	2.0	276	41.0	100.0	337.1	14.8
Integrated age ± 1s			n=18		121.9		K2O=7.60 %		333.6	1.1
Plateau ± 1s		steps E-R	n=14	MSWD=0.79					**334.9**	**0.9**

APPENDIX 1
(continued)

ID	Power (Watts)	$^{40}Ar/^{39}Ar$	$^{37}Ar/^{39}Ar$	$^{36}Ar/^{39}Ar$ (x 10^{-3})	$^{39}Ar_K$ (x 10^{-15} mol)	K/Ca	$^{40}Ar^*$ (%)	^{39}Ar (%)	Age (Ma)	±1s (Ma)
SZX-23A biotite, 0.97 mg, J=0.0161535										
A	650	5.640	0.0333	3.655	9.7	15	80.8	2.2	127.6	1.2
B	750	13.31	0.0046	0.341	31.8	110	99.2	9.6	348.2	1.0
C	850	12.85	0.0016	0.182	76.2	319	99.6	27.3	338.4	0.5
D	920	13.05	0.0038	0.293	38.2	134	99.3	36.2	342.5	0.6
E	1000	12.95	0.0103	0.199	35.2	49	99.6	44.4	340.8	0.6
F	1075	13.22	0.0055	0.122	75.3	92	99.7	61.9	347.6	0.6
G	1110	13.07	0.0033	0.130	55.9	156	99.7	74.9	344.1	1.1
H	1180	12.92	0.0074	0.264	46.8	69	99.4	85.8	339.5	0.8
I	1210	12.90	0.0086	0.160	30.2	59	99.6	92.8	339.6	0.7
J	1250	12.89	0.0312	0.299	18.6	16	99.3	97.1	338.6	0.8
K	1300	12.89	0.1021	0.323	6.6	5	99.3	98.6	338.6	1.2
L	1650	14.41	0.0399	5.515	5.9	13	88.7	100.0	338.1	1.7
Integrated age ± 1s			n=12		430.4		K2O=10.55 %		337.8	0.5
Plateau ± 1s		steps B-K	n=10	MSWD=24.27					**341.6**	**1.1**
SZX-24 biotite, 0.49 mg, J=0.0163386										
A	650	11.45	0.0517	5.680	14.6	10	85.3	2.8	266.7	1.6
B	750	13.10	0.0052	0.372	74.8	99	99.2	17.4	346.6	1.4
C	850	12.70	0.0016	0.194	121.9	321	99.5	41.1	338.1	0.8
D	920	12.89	0.0038	0.192	45.9	136	99.6	50.1	342.8	0.8
E	1000	12.94	0.0035	0.252	61.4	145	99.4	62.1	343.7	0.6
F	1075	12.71	0.0026	0.195	89.0	194	99.5	79.4	338.5	0.9
G	1110	12.76	0.0042	0.260	44.4	120	99.4	88.0	339.1	0.6
H	1180	12.74	0.0327	0.572	33.9	16	98.7	94.6	336.4	1.1
I	1210	13.01	0.2562	0.961	8.4	2	98.0	96.3	340.8	1.4
J	1250	13.02	0.2630	1.153	8.3	2	97.5	97.9	339.6	1.4
K	1300	13.71	0.1085	2.533	7.8	5	94.6	99.4	346.2	1.4
L	1650	36.59	0.0200	81.258	3.0	25	34.3	100.0	336.6	7.5
Integrated age ± 1s			n=12		513.4		K2O=24.63 %		338.7	0.5
Plateau ± 1s		steps B-L	n=11	MSWD=10.74					**340.9**	**0.9**
SZX-24 muscovite, 0.39 mg, J=0.0162481										
A	600	12.93	0.1943	15.17	1.3	3	65.4	0.6	231.8	21.1
B	650	16.65	0.0454	9.19	1.3	11	83.7	1.2	367.8	19.3
C	700	14.09	0.0137	2.70	1.5	37	94.3	1.9	352.2	17.7
D	750	14.18	0.0047	1.79	3.9	109	96.3	3.6	360.7	7.0
E	800	13.36	0.0037	0.80	6.6	138	98.2	6.6	348.2	4.1
F	840	13.06	0.0018	0.74	11.7	284	98.3	11.9	341.2	2.7
G	880	12.94	0.0014	0.63	20.1	356	98.6	21.0	339.1	1.5
H	920	12.81	0.0006	0.45	45.6	826	99.0	41.7	337.2	0.9
I	960	12.73	0.0006	0.33	37.3	925	99.2	58.5	336.2	1.5
J	1000	12.77	0.0006	0.65	20.4	868	98.5	67.8	334.9	1.5
K	1040	12.81	0.0013	0.54	15.1	385	98.7	74.6	336.7	1.9
L	1080	12.73	0.0013	0.49	18.1	381	98.9	82.8	334.9	1.7
M	1120	12.83	0.0008	0.55	19.5	629	98.7	91.6	337.1	1.7
N	1160	13.41	0.0051	2.99	6.3	100	93.4	94.4	333.6	4.1
O	1200	13.60	0.0105	2.00	2.8	48	95.6	95.7	345.2	9.1
P	1250	20.67	0.0575	26.85	1.8	9	61.6	96.5	338.8	14.7
Q	1350	13.46	0.0545	1.76	3.2	9	96.2	98.0	343.7	7.8
R	1650	22.22	0.0120	32.42	4.5	42	56.8	100.0	336.4	7.1
Integrated age ± 1s			n=18		221.1		K2O=13.40 %		337.5	0.7
Plateau ± 1s		steps F-R	n=13	MSWD=0.87					**336.9**	**0.5**
O-1 biotite, 0.32mg, J=0.0161889										
A	650	11.77	0.0052	4.870	29.1	97	87.8	4.5	278.5	0.9
B	750	12.81	0.0014	0.449	113.0	360	99.0	22.0	336.1	0.5
C	850	12.64	0.0008	0.212	149.6	669	99.5	45.2	333.8	0.5
D	920	12.72	0.0017	0.231	49.4	308	99.5	52.9	335.6	0.5
E	1000	12.73	0.0017	0.358	62.3	295	99.2	62.6	335.0	0.6
F	1075	12.62	0.0012	0.232	128.1	440	99.5	82.4	333.1	0.7
G	1110	12.67	0.0017	0.315	46.8	301	99.3	89.7	333.6	0.6
H	1180	12.78	0.0044	0.622	32.7	116	98.6	94.7	334.2	0.6
I	1210	12.78	0.0312	0.568	11.6	16	98.7	96.5	334.7	1.0
J	1250	12.84	0.1799	0.468	5.8	3	99.0	97.5	337.2	1.5
K	1300	12.88	0.0056	0.413	16.4	91	99.1	100.0	338.0	0.8
Integrated age ± 1s			n=11		644.8		K2O=8.16 %		332.0	0.4
Plateau ± 1s		steps B-I	n=8	MSWD=4.92					**334.9**	**0.4**

APPENDIX 1
(continued)

ID	Power (Watts)	$^{40}Ar/^{39}Ar$	$^{37}Ar/^{39}Ar$	$^{36}Ar/^{39}Ar$ (x 10^{-3})	$^{39}Ar_K$ (x 10^{-15} mol)	K/Ca	$^{40}Ar^*$ (%)	^{39}Ar (%)	Age (Ma)	±1s (Ma)
Integrated age ± 1s			n=11		644.8		K2O=8.16 %		332.0	0.4
Plateau ± 1s		steps B-I	n=8	MSWD=4.92					**334.9**	**0.4**
O-3 biotite, 0.61 mg, J=0.0162555										
A	650	9.76	0.1808	15.912	4.7	3	51.9	3.0	142.4	2.8
B	750	13.04	0.1100	2.094	9.4	5	95.3	8.9	331.3	1.2
C	850	12.96	0.0425	0.977	13.9	12	97.8	17.7	337.4	0.8
D	920	13.10	0.0804	1.140	10.4	6	97.5	24.3	339.6	0.7
E	1000	13.05	0.0810	0.605	16.9	6	98.7	34.9	342.3	0.9
F	1075	12.90	0.0294	0.314	38.9	17	99.3	59.6	340.7	0.7
G	1110	12.86	0.0379	0.439	22.7	13	99.0	74.0	338.8	0.7
H	1180	12.73	0.0729	0.447	27.9	7	99.0	91.6	335.6	0.6
I	1210	12.75	0.5645	0.620	7.2	1	98.9	96.2	336.0	1.2
J	1250	12.96	0.5567	0.930	4.5	1	98.2	99.0	338.7	1.6
K	1300	13.36	0.1535	1.962	1.6	3	95.7	100.0	340.2	3.3
Integrated age ± 1s			n=11		157.9		K2O=6.12 %		332.92	0.49
Plateau ± 1s		steps B-K	n=10	MSWD=11.18					**338.2**	**0.9**
O-4 muscovite, 0.38 mg, J=0.0163193										
A	600	19.76	0.1572	36.21	3.3	3	45.8	1.2	248.4	4.3
B	650	13.85	0.0490	0.10	3.5	10	99.8	2.5	366.3	2.5
C	700	13.99	0.0088	2.22	4.9	58	95.3	4.3	354.7	1.8
D	750	13.49	0.0039	1.07	14.9	130	97.6	9.7	350.8	1.5
E	800	13.09	0.0028	0.68	20.2	185	98.5	17.1	343.9	0.8
F	840	12.92	0.0020	0.47	29.0	257	98.9	27.8	341.2	0.7
G	880	12.82	0.0015	0.32	39.0	351	99.3	42.1	339.7	0.7
H	920	12.62	0.0011	0.13	51.5	455	99.7	61.1	336.2	0.8
I	960	12.70	0.0011	0.31	43.7	473	99.3	77.1	337.0	0.7
J	1000	12.83	0.0010	0.33	31.7	526	99.2	88.8	339.9	0.9
K	1040	12.83	0.0025	0.34	14.8	204	99.2	94.2	339.8	0.9
L	1080	12.86	0.0031	0.82	9.0	164	98.1	97.5	337.2	1.2
M	1120	12.93	0.0086	0.91	4.9	59	97.9	99.4	338.1	1.7
O	1200	12.54	0.0409	0.93	0.8	12	97.8	99.7	328.6	8.2
P	1250	12.85	0.1769	1.93	0.9	3	95.7	100.0	329.2	7.3
Integrated age ± 1s			n=15		272.0		K2O=16.85 %		339.1	0.5
Plateau ± 1s		steps H-M	n=6	MSWD=3.3					**337.9**	**0.7**
O-6 muscovite, 0.22 mg, J=0.015										
A	600	15.65	0.1872	28.69	2.6	3	45.9	1.1	184.2	4.2
B	650	12.41	0.0591	3.65	1.6	9	91.3	1.8	282.8	4.8
C	700	13.42	0.0322	3.17	1.6	16	93.0	2.5	309.1	3.6
D	750	13.36	0.0078	1.14	4.1	66	97.5	4.2	321.3	1.8
E	800	13.43	0.0048	1.48	5.6	107	96.7	6.6	320.6	1.6
F	840	13.13	0.0016	0.96	9.5	327	97.8	10.6	317.4	1.2
G	880	12.91	0.0021	0.51	16.0	238	98.8	17.4	315.3	0.8
H	920	12.77	0.0009	0.30	63.1	549	99.3	44.1	313.6	1.2
I	960	12.62	0.0005	0.23	75.4	1118	99.5	76.1	310.7	1.0
J	1000	12.92	0.0009	0.59	24.6	580	98.7	86.5	314.9	0.9
K	1040	12.97	0.0018	0.70	12.5	287	98.4	91.8	315.5	0.7
L	1080	12.96	0.0023	0.33	6.4	219	99.3	94.5	317.7	1.4
M	1120	13.68	0.0116	3.76	3.1	44	91.9	95.8	311.0	2.5
N	1160	13.55	0.0120	2.61	2.0	43	94.3	96.6	315.8	3.5
O	1200	13.49	0.0642	2.03	1.4	8	95.6	97.2	318.4	5.1
P	1250	13.57	0.2113	3.11	1.3	2	93.3	97.7	313.4	5.5
Q	1350	13.50	0.4429	2.21	3.3	1	95.4	99.1	318.3	2.4
R	1650	20.39	0.0135	29.25	2.0	38	57.6	100.0	292.3	5.9
Integrated age ± 1s			n=18		236.1		K2O=27.48 %		311.9	0.6
Plateau ± 1s		steps H-O	n=8	MSWD=3.63					**314.4**	**0.8**

Notes: Isotopic ratios corrected for blank, radioactive decay, and mass discrimination, not corrected for interferring reactions
Errors quoted for individual analyses include analytical error only, without interfering reaction or J uncertainties
Integrated age calculated by recombining isotopic measurements of all steps
Integrated age error calculated by recombining errors of isotopic measurements of all steps
Plateau age is inverse-variance-weighted mean of selected steps
Plateau age error is inverse-variance-weighted mean error (Taylor, 1982) times root MSWD where MSWD > 1
Plateau and integrated ages incorporate uncertainties in interferring reaction corrections and J factors
Decay constants and isotopic abundances after Steiger and Jaeger (1977)